

Department of Physics and Astronomy  
University of Heidelberg

Bachelor Thesis in Physics  
submitted by

**Fabian Zhou**

born in Frankfurt/Main (Germany)

**2019**



# Bogoliubov theory of dilute Bose Einstein condensates with a background flow

This Bachelor Thesis has been carried out by Fabian Zhou at the  
Kirchhoff-Institute of Physics in Heidelberg  
under the supervision of  
Prof. Thomas Gasenzer



## Abstract

We study a one component Bose Einstein condensate, in which we realise an acoustic event horizon in a step-like configuration. In this process we make use of the microscopic Bogoliubov theory for dilute Bose Einstein condensates. We investigate density correlations of scattering processes at the horizon. This results in long-range correlation signals, which can be identified with an analogue Hawking-effect. Furthermore, we give a brief insight into analogue gravity and derive the acoustic metric.

Subsequently, we consider a two component Bose Einstein condensate with an additional tunnel coupling. We assume both components to have an opposite background flow leading to a strong coupling between the symmetric and the antisymmetric degrees of freedom. For this theoretical setup the dispersion relation is derived and its behaviour analysed.

## Zusammenfassung

Wir studieren ein einkomponentiges Bose-Einstein-Kondensat, in dem wir in einer stufenartigen Konfiguration einen akustischen Ereignishorizont realisieren. Dabei machen wir Gebrauch von der mikroskopischen Bogoliubov-Theorie für verdünnte Bose-Einstein-Kondensate. Wir untersuchen Dichtekorrelationen von Streuprozessen am Horizont. Dies führt zu Langstreckenkorrelationssignalen, welche wir mit einem analogen Hawking-Effekt identifizieren können. Desweiteren geben wir einen kurzen Einblick in die Gravitationsanalogie und leiten die akustische Metrik her.

Darauffolgend betrachten wir ein zweikomponentiges Bose-Einstein-Kondensat mit zusätzlicher Tunnelkopplung. Wir setzen voraus, dass beide Komponenten einen entgegengesetzten Hintergrundfluss haben. Dies führt dazu, dass die symmetrischen und antisymmetrischen Freiheitsgrade stärker gekoppelt sind. Für diese theoretische Konfiguration leiten wir die Dispersionsrelation her und analysieren ihr Verhalten.



# Contents

<b>1</b>	<b>Introduction</b>	<b>1</b>
1.1	Motivation . . . . .	1
1.2	Experimental Situation . . . . .	2
<b>2</b>	<b>Theoretical background</b>	<b>4</b>
2.1	Bogoliubov theory of a one component Bose Einstein condensate with a background flow . . . . .	4
2.2	The acoustic metric . . . . .	9
2.3	Quantum fluctuations around an acoustic black hole horizon . . . . .	11
2.3.1	Step-like background configuration . . . . .	11
2.3.2	Dispersion relation and the different $k$ -roots . . . . .	12
2.3.3	Matching conditions at the horizon . . . . .	15
2.3.4	The scattering solution . . . . .	16
2.3.5	Quantisation . . . . .	21
<b>3</b>	<b>Density correlations</b>	<b>23</b>
<b>4</b>	<b>Modifying the two component model</b>	<b>28</b>
4.1	Bogoliubov theory of a two-component Bose Einstein condensate with opposite background flows . . . . .	28
4.2	Dispersion relation . . . . .	32
<b>5</b>	<b>Conclusion</b>	<b>38</b>
5.1	Outlook . . . . .	39
	<b>References</b>	<b>42</b>
	<b>Eidesstattliche Erklärung</b>	<b>44</b>

## List of Figures

2.1	Dispersion relation for upstream and downstream region . . . . .	14
2.2	U scattering mode . . . . .	16
2.3	D1 scattering mode . . . . .	17
2.4	D2 scattering mode . . . . .	17
2.5	Scattering coefficients for all incoming channels . . . . .	20
3.1	Density correlation function . . . . .	26
4.1	Background density $n_0(x)$ . . . . .	30
4.2	Different branches of the dispersion relation . . . . .	36
4.3	Power law of the dispersion relation . . . . .	36
4.4	Different modes for fixed frequency $k$ . . . . .	37

# 1 Introduction

## 1.1 Motivation

The theory of general relativity by A. Einstein (1915) is currently the most fundamental theory in terms of gravity. It states that gravity is a basic property linked to curvature of space-time, caused by mass and energy. An essential part of general relativity are the so called Einstein's field equations, which are ten equations of motion describing the interaction of mass with the underlying space time. Amongst other solutions, the "black hole" emerges as one of the strangest and most intriguing predictions. These objects consists of a tremendous amount of compressed matter resulting in a gravitational field strong enough, that nothing can escape once the event horizon is crossed. Consequently it was thought for a long time that it is not possible to directly observe such a black hole, since not even light is able to escape it.

The turning point was brought years later by Stephen Hawking et al. By comparison of the thermodynamic laws with the properties of a black hole, he concluded that black holes must have a finite temperature (Hawking-temperature). Subsequently they have to emit a continuous flux of thermal radiation. This was confirmed by Hawking in 1974 [1], where he investigated quantum mechanical effects in curved space time. As was shown, the Hawking-temperature is inversely proportional to the mass resulting in a very low temperature, much smaller than the cosmic microwave background of approximately  $2.7K$ . For this reason, it has not been possible to detect this thermal radiation yet.

Later on in 1981, William G. Unruh investigated models of analogue gravity, which consists of analogies (often based on condensed matter physics) to probe aspects of the physics of curved spacetime [2]. He recognised the similarities of sound waves propagating through non-homogeneous media and light propagating in curved space time. In addition, a transition from a subsonic to a supersonic flow creates an acoustic horizon which influences the sound waves in the same way a black hole event horizon affects photons [3]. In this context the analogue black hole is called "dumb hole".

Much earlier in 1972, he used a vivid example of fish living near a waterfall to clarify the circumstances around such a horizon [4]. For the fish the waterfall at the edge of their habitat was a point of no return, since the supersonic flow velocity of the the water becomes too large. Furthermore the screams of those who travelled too close to the horizon were bass shifted (similar to the Doppler-shift), which means that the wave length of the sound waves become larger for an observing fish above the waterfall, and no fish could be heard from beyond the horizon.

Unruh even realised that the equations of motion of sound waves and those around the event horizon are identical [3]. Also the quantisation of these sound waves would result in thermal radiation, just as Hawking had predicted in the case of black hole horizons.

## 1.2 Experimental Situation

Due to these theoretical results, the experiments investigating Hawking-like effects accumulated in the last decade. There was for instance a classical analogue setup involving moving water in a tank [5], where a dumb hole configuration was realised and the Hawking effect observed. In other cases light pulses moving in optical fibers [6] or lasers travelling in a non-linear luminous liquid were used to realise a sonic horizon [7]. The problem considered in this thesis is an analogue transsonic system in a Bose Einstein condensate, whose theory has been worked out well by now. From the experimental point of view, the manipulation of ultracold atomic gases and the control of their physical properties became more familiar over the last decades. Currently, one of the most significant publications is by Jeff Steinhauer from the Israel Institute of Technology in 2015, where he stated that the analogue quantum Hawking radiation and its entanglement were observed [8].

Steinhauer used a BEC of  $^{87}\text{Rb}$  confined by a radial laser, such that the behaviour is quasi one dimensional. Another laser is used to create a very sharp potential which constitutes the acoustic horizon. Hence the resulting velocity gradient is chosen to be very steep in order to maximise the Hawking temperature and facilitate the observation of Hawking radiation. In order to achieve a background flow velocity the potential step is swept along the condensate. To this end, all considerations are made in the rest frame of the horizon.

However, Steinhauer's paper got strong criticism, especially by Ulf Leonhardt, who directly picked up on Steinhauer's work in his publication "Questioning the recent observation of quantum Hawking radiation" [9]. Apparently, one of the main flaws was the inconsistency between the theory and the measurements on the one hand, and the incompleteness of data on the other hand. For instance, Steinhauer claimed that the population of Hawking-partners inside the black hole was measured, yet the corresponding data was not published. Moreover, no measurement of the velocity gradient was reported, which seems to be significant if one considers a system including an analogue of an event horizon.

Another point of criticism by Leonhardt was the quality of Steinhauer's fit functions. In the plot of the measured Hawking population the distribution is stated to be planckian, whereas a linear fit would have a similar fit accuracy. Accordingly this fit is no longer very convincing, as well as the confidence of  $5.7\sigma$  for the observation of entanglement. All in all the analysis of Steinhauer's paper "raises severe doubts on the observation of Hawking radiation" [9]. Steinhauer defended himself in another publication and contradicts each point of Leonhardt, whereby it becomes difficult to assess Steinhauer's work.

Nevertheless, in 2018 he again published a paper on exactly the same topic. The experimental setup was improved and the errors minimised. While Leonhardt remains

sceptical, there are supporters like the theoretical physicist Renaud Parentani, who deals with the theoretical side of analogue Hawking radiation. According to him, "Jeff [Steinhauer] is really, at the moment, the world-leading expert of using cold atoms to probe black hole physics".

In section 2 we consider a one component Bose Einstein condensate with a step-like configuration in order to reach a sonic horizon. Applying the Bogoliubov approach, we derive the dispersion relation, which is the basic object for expressing our fields in an appropriate way. To this end, we take a closer look at scattering at the horizon, where we consider free particle excitations initiating the scattering process. The actual Hawking radiation originates from virtual pair production. Naively said, one particle of the pair with positive energy escapes the black hole, while the negative energy partner falls into the black hole. In our analogue model these partners are represented by the outgoing modes of the scattering process. For the purpose of clarifying the gravitational analogy, the acoustic metric is deduced in the hydrodynamic approximation.

In the following section long-range correlations are computed, which can be identified with an analogue Hawking effect.

These derivations were also shown for a Bose Einstein condensate with two components [10]. The results are very similar compared to the case of one component.

However, in the last section we consider the model of two components with modified conditions. In this case the two components have an opposite background flow velocity. Further there is an additional tunnelling term in the Hamiltonian of this configuration, depending on the tunnel coupling constant  $J$ . Therefore a circulating current of the condensate arises. This theoretical setup was motivated by the idea that it could be easier to handle in an experiment. Steinhauer's experiment for example is somehow restricted, since the condensate is spatially limited and therefore the potential step cannot be swept along forever. To this end, Steinhauer had to redo his experiments often. It is clear that with each run the initial conditions are always slightly altered, which reduces the accuracy. Whether one can counteract this fact with enough repetitions, is questionable. In contrast, the centre of the circulating flow would be stationary and the dynamics could be observed for a much longer time.

However, it turns out that the system becomes much more complicated, more precisely, the degrees of freedom are more strongly coupled. Under certain approximations it is possible to derive a dispersion relation, which unfortunately does not resemble one which reproduces the Hawking-effect. Nevertheless there is a band like structure which is interesting from a condensed matter point of view.

Throughout the whole thesis we work in natural units, i.e.  $\hbar = 1$ .

## 2 Theoretical background

### 2.1 Bogoliubov theory of a one component Bose Einstein condensate with a background flow

We consider a system of a one component Bose Einstein condensate in one spatial dimension described by the following Hamiltonian:

$$\mathcal{H} = \int dx \left\{ \psi^\dagger \left[ -\frac{1}{2m} \partial_x^2 + (V(x) - \mu) \right] \psi + \frac{g}{2} \psi^\dagger \psi^\dagger \psi \psi \right\}, \quad (2.1)$$

with an external potential  $V(x)$ , the chemical potential  $\mu$  and the coupling constant  $g$ . The bosonic annihilation and creation operator  $\psi$  and  $\psi^\dagger$  fulfil the usual commutation relations for fixed time

$$[\psi(x, t), \psi^\dagger(x', t)] = \delta(x - x'), \quad (2.2)$$

whilst all other commutation relations vanish. Using the Heisenberg equation of motion

$$i\partial_t \psi = [\psi, \mathcal{H}], \quad (2.3)$$

we obtain the equations of motion for the condensate, which is the Gross-Pitaevskii equation (GPE)

$$i\partial_t \psi = \left[ -\frac{1}{2m} \partial_x^2 + (V(x) - \mu) + g|\psi|^2 \right] \psi, \quad (2.4)$$

and an analogous equation for  $\psi^\dagger$ .

Now we consider the so called Madelung transformation for our field operators, which expresses them in terms of their real-valued density  $n(x)$  and phase  $\theta(x)$

$$\psi(x) = \sqrt{n(x)} e^{i\theta(x)}, \quad (2.5)$$

where  $n$  and  $\theta$  also obey the commutation relation

$$[n(x, t), \theta(x', t)] = i\delta(x - x'). \quad (2.6)$$

Inserting the transformation (2.5) in the GPE (2.4) leads to coupled equations of motion for  $n$  and  $\theta$

$$\partial_t n = -\frac{1}{m} \partial_x [n \partial_x \theta], \quad (2.7a)$$

$$\partial_t \theta = \frac{1}{2m} \frac{\partial_x^2 \sqrt{n}}{\sqrt{n}} - \frac{1}{2m} (\partial_x \theta)^2 - [V(x) - \mu] - gn. \quad (2.7b)$$

Equation (2.7a) is the continuity equation, equation (2.7b) is equivalent to the quantum Euler equation for fluids, featuring the quantum pressure term (first term on the r.h.s.). Since we are in the quasi-condensate regime, the Bogoliubov approach is appropriate. Hence we use the mean field approach, where we consider our fields as a smooth background with small fluctuations on them,

$$n(x, t) = n_0(x) + \delta n(x, t), \quad (2.8a)$$

$$\theta(x, t) = \theta_0(x) + \delta \theta(x, t). \quad (2.8b)$$

In the following we will leave out the position- and time-dependence of these fields. The background flow velocity of our condensate is defined as

$$v(x) := \frac{\partial_x \theta_0(x)}{m}. \quad (2.9)$$

Linearising the equations (2.7) we find in to lowest order

$$\left[ -\frac{1}{2m} \partial_x^2 + \frac{1}{2} m v^2 + V(x) - \mu + g n_0 \right] \sqrt{n_0} = 0, \quad (2.10)$$

which is again the GPE with an additional kinetic energy term  $\frac{1}{2} m v^2$  due to the background flow velocity. Moreover we find

$$\partial_x [n_0 v] = 0, \quad (2.11)$$

which is the continuity equation for the time-independent case.

To first order we find a set of two coupled equations of motion

$$\partial_t \delta n = -\partial_x \left[ \delta n v + \frac{n_0}{m} \partial_x \delta \theta \right], \quad (2.12a)$$

$$\partial_t \delta \theta = -v \partial_x \delta \theta + \frac{1}{4m n_0} \partial_x \left[ n_0 \partial_x \left( \frac{\delta n}{n_0} \right) \right] - g \delta n. \quad (2.12b)$$

As seen in [11], we now introduce new variables  $\delta \tilde{n} = \frac{\delta n}{\sqrt{n_0}}$  and  $\delta \tilde{\theta} = \delta \theta \sqrt{n_0}$ , to simplify the notation.  $\delta \tilde{n}$  and  $\delta \tilde{\theta}$  now have the same dimension. Now the equations of motion (2.12a) and (2.12b) take the compact form

$$[\partial_t + v \partial_x] \delta \tilde{n} = \frac{1}{m} \partial_x^2 \delta \tilde{\theta}, \quad (2.13a)$$

$$[\partial_t + v \partial_x] \delta \tilde{\theta} = \left[ \frac{1}{4m} \partial_x^2 - g n_0 \right] \delta \tilde{n}, \quad (2.13b)$$

If we now consider a homogeneous region of the condensate (which means  $n_0, v = \text{const.}$  and  $V(x) = 0$ ), we can expand the solution of equations (2.11) in terms of plane waves

$$\delta \tilde{n} = A e^{i(kx - \omega t)}, \quad \delta \tilde{\theta} = B e^{i(kx - \omega t)}, \quad (2.14)$$

where  $A$  and  $B$  are constant amplitudes. Substituting these into equations (2.12a) and (2.12b) leads to a matrix equation

$$\begin{pmatrix} -i(\omega - vk) & \frac{1}{m} k^2 \\ \frac{1}{4m} k^2 + g n_0 & -i(\omega - vk) \end{pmatrix} \times \begin{pmatrix} A \\ B \end{pmatrix} = 0. \quad (2.15)$$

In order for this matrix equation to have nontrivial solutions for the amplitudes the determinant of the matrix has to vanish. This leads to the dispersion relation for our system

$$(\omega - vk)^2 = c^2 k^2 \left( \frac{1}{4} \xi^2 k^2 + 1 \right), \quad (2.16)$$

with the speed of sound  $c^2 = \frac{g n_0}{m}$  and the healing length  $\xi = \frac{1}{m c}$ .

The r.h.s. of this dispersion relation is the standard Bogoliubov dispersion, which is linear in the low  $k$  limit and quadratic for large  $k$ . On the l.h.s. there is an energy shift due to the background flow with velocity  $v$  which can be seen as a Doppler-shift.

Following the Bogoliubov approach explained in [12], we know there is the quasi particle basis in which the second order Hamiltonian (second order considering the fluctuations) becomes diagonal

$$\mathcal{H}^{(2)} = \sum_k \omega_k \hat{b}_k \hat{b}_k^\dagger, \quad (2.17)$$

with the annihilation and creation operator  $\hat{b}_k$  and  $\hat{b}_k^\dagger$  for bosonic quasi-particle excitations. They fulfil the bosonic commutation relations

$$[\hat{b}_k, \hat{b}_{k'}^\dagger] = \delta_{kk'}, \quad (2.18)$$

whilst again the others vanish. Therefore we expand our fields  $\delta\tilde{n}$  and  $\delta\tilde{\theta}$  in terms of the quasi-particle operators, this is called the Bogoliubov expansion [11]. Thus we get

$$\delta\tilde{n}(x, t) = \sum_k \left[ f_k^+(x) e^{-i\omega_k t} \hat{b}_k + \left( f_k^+(x) \right)^* e^{i\omega_k t} \hat{b}_k^\dagger \right], \quad (2.19a)$$

$$\delta\tilde{\theta}(x, t) = -i \sum_k \left[ f_k^-(x) e^{-i\omega_k t} \hat{b}_k - \left( f_k^-(x) \right)^* e^{i\omega_k t} \hat{b}_k^\dagger \right]. \quad (2.19b)$$

The mode functions  $f_k^\pm$  are related to the normal Bogoliubov mode functions  $u_k$  and  $v_k$  via  $f_k^\pm = u_k \pm v_k$ . The normal mode functions  $u_k$  and  $v_k$  are normalised by

$$\int dx \left[ |u_k(x)|^2 - |v_k(x)|^2 \right] = \pm 1, \quad (2.20)$$

Therefore the mode functions  $f_k^\pm$  are normalised to

$$\frac{1}{2} \int dx \left[ \left( f_k^+(x) \right)^* \left( f_{k'}^-(x) \right) + \left( f_k^-(x) \right)^* \left( f_{k'}^+(x) \right) \right] = \pm \delta_{k,k'} \quad (2.21)$$

In this normalisation the negative sign of the Kronecker-delta arises from the negative norm branch of the dispersion relation, which will be specified later. If we now insert the Bogoliubov expansions (2.19) in the equations of motion (2.13) we get the equations for the eigenmodes  $f_k^\pm$  and their corresponding eigenvalues  $\tilde{\Omega}_k$

$$\mathcal{L} \begin{pmatrix} f_k^+ \\ f_k^- \end{pmatrix} = \tilde{\Omega}_k \begin{pmatrix} f_k^+ \\ f_k^- \end{pmatrix}, \quad (2.22)$$

with  $\tilde{\Omega}_k = \omega_k + iv\partial_x$  and

$$\mathcal{L} = \begin{pmatrix} 0 & \frac{1}{m}\partial_x^2 \\ \frac{1}{4m}\partial_x^2 - gn_0 & 0 \end{pmatrix}. \quad (2.23)$$

It should be mentioned that the operator  $\mathcal{L}$  has a more general expression [13]. However, for our case of a one component condensate, where we made use of transformation (2.5), it reduces to (2.23).

The solutions for equation (2.22), under the condition that the condensate is homogeneous, are

$$f_k^+(x) = e^{ikx} F_k^+ = e^{ikx} \frac{\frac{k^2}{m}}{\sqrt{\left| \operatorname{Re} \left( \frac{k^2}{2m} \Omega_k^* \right) \right|}}, \quad (2.24a)$$

$$f_k^-(x) = e^{ikx} F_k^- = e^{ikx} \frac{\Omega_k}{\sqrt{\left| \operatorname{Re} \left( \frac{k^2}{2m} \Omega_k^* \right) \right|}}, \quad (2.24b)$$

with  $\Omega_k = \omega_k - vk$ , [11].

Since it is possible that  $k$  is complex, the normalisation factor  $\left| \operatorname{Re} \left( \frac{k^2}{2m} \Omega_k^* \right) \right|^{-\frac{1}{2}}$  ensures that the normalisation condition (2.21) is still fulfilled. This is easy to check by inserting for  $f_k^\pm(x)$  in the normalisation condition (2.21).

If we now look at the normalisation (2.21), we see that there are modes belonging to the positive and the negative norm branch. This corresponds to a positive and a negative co-moving frequency, respectively. Because of the fourth order polynomial of the dispersion relation, there seems to be a symmetry, such that for every wave vector  $k$  and the associated frequency  $\omega(k)$  there is a  $-k$  with corresponding  $-\omega(k)$ . As a result, we can replace the sum over the wave vector  $k$  in the expansions (2.19) with an integral over the frequency  $\omega$ , restricted to  $\omega > 0$ . Consequently, one has to take the Jacobian  $\left| \frac{dk}{d\omega} \right|$  into account, which is the inverse of the group velocity  $v_g = \frac{d\omega}{dk}$ . It is important that beside the integral over  $\omega$ , one also has to sum over all possible  $k$ -roots for each frequency  $\omega$ . Otherwise not all modes summed over in equation (2.19) would be taken into account. Therefore our new mode functions are

$$f_l^+(x, \omega) = e^{ik_l x} F_l^+(\omega) = e^{ik_l x} \frac{\frac{k_l^2}{m}}{\sqrt{|v_g(k_l)| \left| \operatorname{Re} \left( \frac{k_l^2}{2m} \Omega_l^* \right) \right|}}, \quad (2.25a)$$

$$f_l^-(x, \omega) = e^{ik_l x} F_l^-(\omega) = e^{ik_l x} \frac{\Omega_l}{\sqrt{|v_g(k_l)| \left| \operatorname{Re} \left( \frac{k_l^2}{2m} \Omega_l^* \right) \right|}}. \quad (2.25b)$$

In the above relations the index  $l$  labels one of the four  $k$ -roots for fixed frequency  $\omega$ . Additionally, we also rescale our quasi-particle operators as follows

$$\hat{b}_k = \frac{\hat{b}_{k_l}(\omega)}{\sqrt{|v_g(k_l)|}}. \quad (2.26)$$

The normalisation now becomes

$$\frac{1}{2} \int dx \left[ (f_l^+(x, \omega))^* (f_{l'}^-(x, \omega')) + (f_l^-(x, \omega))^* (f_{l'}^+(x, \omega')) \right] = \pm \delta_{l,l'} \delta(\omega - \omega'), \quad (2.27)$$

and the Bogoliubov expansion reads

$$\delta \tilde{n}(x, t) = \int_0^\infty d\omega \sum_l \left[ f_l^+(x, \omega) e^{-i\omega t} \hat{b}_l(\omega) + (f_l^+(x, \omega))^* e^{i\omega t} \hat{b}_l^\dagger(\omega) \right], \quad (2.28a)$$

$$\delta \tilde{\theta}(x, t) = -i \int_0^\infty d\omega \sum_l \left[ f_l^-(x, \omega) e^{-i\omega t} \hat{b}_l(\omega) - (f_l^-(x, \omega))^* e^{i\omega t} \hat{b}_l^\dagger(\omega) \right]. \quad (2.28b)$$

Now we expressed our fields in a way, which is suitable for further investigations. However, before we take a closer look at the geometry of our system and the dispersion relation, we clarify how the propagation of fields in the condensate is similar to field propagation in curved space time.

## 2.2 The acoustic metric

After introducing the Bogoliubov theory for the one component condensate in a rather general case, we now take a look at analogue gravity. It will be shown how the propagation of (long wavelength) sound waves in the Bose gas can be rewritten in terms of a massless scalar field propagation in curved space-time with an acoustic metric. In our case this scalar field is the velocity potential  $\theta$ , or more precisely the phase perturbation  $\delta\theta$ . As already said in the introduction, this similarity can be seen as a motivation, why the possibility of acoustic black holes and Hawking-like excitations were investigated in the first place.

In this section we will derive the acoustic metric and consequently the line element for the system. Since the metric is not defined in one spatial dimension we will work in  $3 + 1$  dimensions. The equations of motion (2.12a) and (2.12b) stay the same, we only replace  $\partial_x \rightarrow \nabla_x$  and  $v \rightarrow \vec{v}$ , though we drop the vector arrow from now on as simplification.

Because the length scales we consider are much larger than the healing length  $\xi$ , we approximate our system in the hydrodynamic limit, which means that the quantum

pressure can be neglected [14]. That is possible because we assume that the condensate does not vary rapidly in space [4]. The quantum pressure is the first term on the r.h.s. in equation (2.7) which becomes the second term on the r.h.s. in equation (2.12b). Thus we can isolate the density fluctuation  $\delta n$

$$\delta n = -\frac{1}{g}(\partial_t + v\nabla_x)\delta\theta = -\frac{n_0}{mc^2}(\partial_t + v\nabla_x)\delta\theta, \quad (2.29)$$

and insert it in equation (2.12a). This results in a wave equation for the phase fluctuation  $\delta\theta$

$$-(\partial_t + \nabla_x v)\frac{n_0}{mc^2}(\partial_t + v\nabla_x)\delta\theta + \nabla_x\left(\frac{n_0}{m}\nabla_x\delta\theta\right) = 0. \quad (2.30)$$

Following [14], it can be brought in the compact form

$$\partial_\mu(f^{\mu\nu}\partial_\nu\delta\theta) = 0, \quad (2.31)$$

with the  $4 \times 4$ -matrix

$$f^{\mu\nu} = \frac{n_0}{c^2} \begin{pmatrix} -1 & -v^j \\ -v^i & c^2\delta^{ij} - v^i v^j \end{pmatrix}, \quad (2.32)$$

with the usual Lorentz-indices  $\mu$  and  $\nu$  running from 0 to 3. Latin indices go from 1 to 3. We know the d'Alembert operator in curved space-time for a massless scalar field in a pseudo-Riemannian geometry, which is defined as

$$\square := \frac{1}{\sqrt{-g}}\partial_\mu(\sqrt{-g}g^{\mu\nu}\partial_\nu), \quad (2.33)$$

where  $g^{\mu\nu}$  is the inverse of the metric  $g_{\mu\nu}$  and  $g = \det(g_{\mu\nu})$ .

By identifying

$$f^{\mu\nu} = \sqrt{-g}g^{\mu\nu}, \quad (2.34)$$

the equation (2.31) can be written in the form of a curved space wave equation

$$\square\delta\theta = 0, \quad (2.35)$$

that is a Klein-Gordon-equation for a massless scalar field propagating in a space-time described by the metric  $g_{\mu\nu}$ .

From equation (2.34) we can compute

$$\det(f^{\mu\nu}) = (\sqrt{-g})^4 g^{-1} = g \stackrel{!}{=} -\frac{n_0^4}{c^2}, \quad (2.36)$$

where the last step is obtained by simply calculating the determinant of  $f^{\mu\nu}$  from (2.32). Now we can write the explicit expression for the inverse metric  $g^{\mu\nu}$

$$g^{\mu\nu} = \frac{1}{n_0 c} \begin{pmatrix} -1 & -v^j \\ -v^i & c^2 \delta^{ij} - v^i v^j \end{pmatrix}, \quad (2.37)$$

and from that we can derive the metric itself by inverting  $g^{\mu\nu}$

$$g_{\mu\nu} = \frac{n_0}{c} \begin{pmatrix} -(c^2 - v^2) & -v^j \\ -v^j & \delta^{ij} \end{pmatrix}. \quad (2.38)$$

Therefore the acoustic line element is

$$ds^2 = \frac{n_0}{c} \left[ c^2 dt^2 + (dx^i - v^i dt) \delta^{ij} (dx^j - v^j dt) \right]. \quad (2.39)$$

In conclusion we manipulated our equations of motion (2.12a) and (2.12b) such that we obtained a Klein-Gordon equation for a massless scalar field propagating in space-time described by the metric  $g_{\mu\nu}$ . This sets the groundwork for investigating analogue gravity. One should notice, that this analogy is only valid in the hydrodynamic approximation, which holds for small  $k$ , or long wave sound modes, respectively.

## 2.3 Quantum fluctuations around an acoustic black hole horizon

### 2.3.1 Step-like background configuration

Now we establish the geometry of our one dimensional system. In order to obtain an event horizon similar to one in the black hole, the fluid should have a transition from a subsonic ( $v < c$ ) to a supersonic ( $v > c$ ) flow. We want the horizon to be at  $x = 0$ . Since the background flow points in the positive  $x$ -direction, there is an upstream region ( $u$ ) for  $x < 0$  and a downstream region ( $d$ ) for  $x > 0$ . In order to achieve a step-like configuration we set the coupling constant to be given by

$$g(x) = g_u \Theta(-x) + g_d \Theta(x), \quad (2.40)$$

where  $\Theta$  is the Heavyside step function. Hence we have two different speeds of sound for the upstream and the downstream region

$$c_{u,d} = \sqrt{\frac{g_{u,d}n_0}{m}}. \quad (2.41)$$

Recall that the background density  $n_0$  and the background velocity  $v$  is equal for both, the upstream and the downstream region, so the continuity equation is fulfilled throughout the whole system. If we now choose  $g_u$  and  $g_d$ , such that

$$c_u > v > c_d, \quad (2.42)$$

we obtain subsonic flow in the upstream region and a supersonic flow in the downstream region. Therefore an acoustic event horizon arises at  $x = 0$ .

### 2.3.2 Dispersion relation and the different $k$ -roots

Now that we set a transition from a subsonic to a supersonic flow, we can take a closer look at the dispersion relation for both, the upstream and the downstream region.

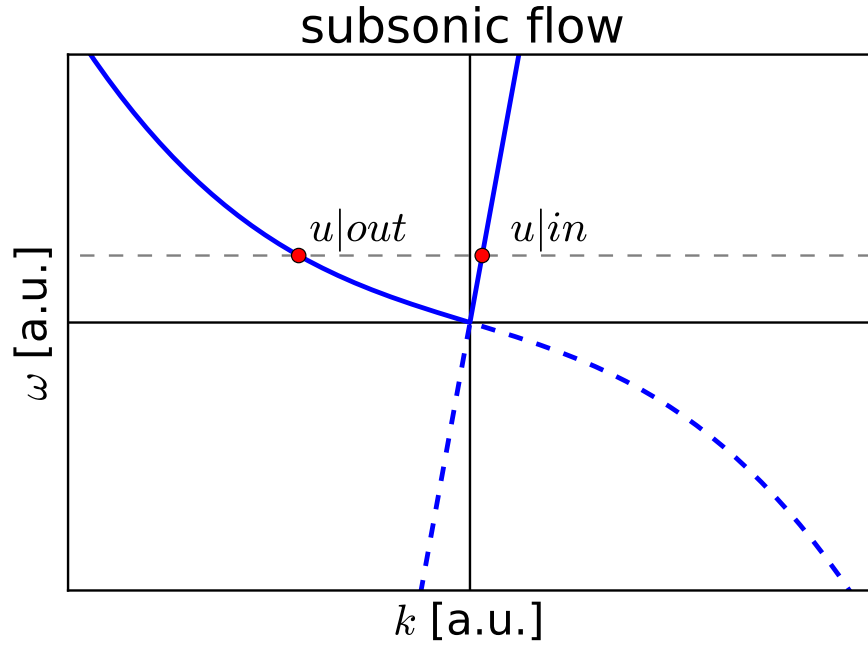
The dispersion relation (2.16) we derived for our system is a fourth order polynomial in  $k$ , consequently there are four (complex) solutions for  $k$  at a fixed frequency  $\omega > 0$ . In addition there is a positive norm branch (solid line) and a negative norm branch (dotted line), corresponding to the two possible signs if one takes the root of equation (2.16). The negative norm branch can be seen as holes or antiparticles, respectively.

In case of a subsonic flow there are two real roots, which we denote by  $k_{u|in}$  and  $k_{u|out}$  (figure 2.1a). “In“ means that the wave vector points towards the horizon and “out“ that it points away from the horizon. They correspond to propagating plane waves and have a positive norm. The other two are complex conjugate to each other and correspond to exponentially growing or decreasing evanescent waves. They have negative norm. Here we discard the one with  $\text{Im}(k_l) > 0$ , since it diverges for  $x \rightarrow -\infty$ . The one we retain is denoted by  $k_{u|eva}$ .

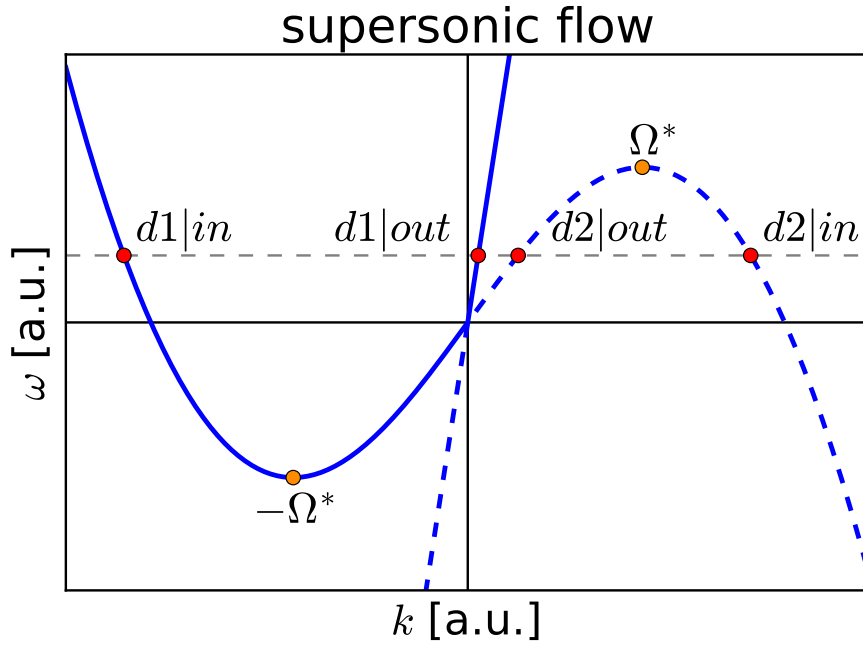
If the flow becomes supersonic, meaning the background flow velocity becomes bigger than the local speed of sound ( $v > c_d$ ), the dispersion is skewed (figure 2.1). Due to the background flow velocity  $v$  the negative norm branch is skewed in a way that a part of it takes positive values for the frequency  $\omega$  and vice versa. Now there exists a certain frequency  $\Omega^* > 0$  where for any  $0 < \omega < \Omega^*$  all four roots are real. The two solutions corresponding to the positive norm branch are denoted by  $k_{d1|in}$  and  $k_{d1|out}$ , whereas the ones in the negative norm branch are denoted by  $k_{d2|in}$  and  $k_{d2|out}$ . Here in and

out means the same, but in this case the in-modes have negative and the out-modes have positive group velocity. Above the critical frequency,  $\omega > \Omega^*$ , there are again two real and two complex roots, more precisely the  $k_{d2|in,d2|out}$  modes do not exist. Instead, there is again the  $k_{d|eva}$  mode after we discard the diverging one.

From now on we use the truncated notation, where we denote the modes only by their index, for instance  $u|in$  means the mode with wave vector  $k_{u|in}$ .



(a) upstream region



(b) downstream region

Figure 2.1: The shifted Bogoliubov dispersion relation (2.16) for a subsonic (a) and a supersonic (b) flow. The positive norm branch is represented by a solid line, whereas the dotted line stands for the negative norm branch. The real solutions for fixed frequency  $\omega$  are marked by red dots. In (b) the critical frequency  $\Omega^*$  is marked by an orange dot, above that there are again two real solutions, [15]

### 2.3.3 Matching conditions at the horizon

We chose our condensate to be homogeneous on both sides of the horizon. The eigenmodes are presented in section 2. However, these eigenmodes are restricted to one side of the horizon so they cannot be the eigenmodes for the whole system. The true eigenmodes of the whole system are linear combinations of the modes (2.25) with appropriate matching at the horizon. Intuitively one expect our fields and their derivatives to be continuous in  $x = 0$ . More rigorously, we obtain the matching conditions by integrating the equations (2.13) over an infinitesimal interval around the horizon. Provided the background flow velocity  $v$  is constant, this results in the matching conditions

$$[\delta\tilde{n}] = 0, \quad (2.43a)$$

$$[\partial_x \delta\tilde{n}] = 0, \quad (2.43b)$$

$$[\delta\tilde{\theta}] = 0, \quad (2.43c)$$

$$[\partial_x \delta\tilde{\theta}] = 0, \quad (2.43d)$$

where the square brackets means  $[\bullet] := [\bullet]_{x \rightarrow 0^+} - [\bullet]_{x \rightarrow 0^-}$ . A detailed derivation of these matching conditions can be seen in [16].

Now, once we have the matching conditions for the field operators, we want to express the conditions in terms of the eigenmodes of the whole system. Therefore we define them as

$$\Pi_r(x, \omega) := \begin{pmatrix} f_r^+(x, \omega) \\ f_r^-(x, \omega) \end{pmatrix}, \quad (2.44)$$

where the index  $r$  indicates which side of the horizon is looked at, so  $r = u$  for  $x < 0$  (upstream) or  $r = d$  for  $x > 0$  (downstream). As was mentioned before the vectors (2.25), which we write as

$$\pi_l(x, \omega) := \begin{pmatrix} f_l^+(x, \omega) \\ f_l^-(x, \omega) \end{pmatrix} = e^{ik_l x} \begin{pmatrix} F_l^+(\omega) \\ F_l^-(\omega) \end{pmatrix}, \quad (2.45)$$

where here  $l$  specifies one of the  $k$ -roots for fixed frequency  $\omega$ , i.e.  $l \in \{u|in, u|out, u|eva, d1|in, d1|out, d2|in, d2|out, d2|eva\}$ , depending on the value of  $\omega$  and which side of the horizon is considered. For instance,  $\Pi_u$  describes an excitation in the upstream region and is a linear combination of  $\pi_{u|in}$ ,  $\pi_{u|out}$ ,  $\pi_{u|eva}$ . By the use of the new definitions (2.44) and (2.45) we are now able to formulate the matching conditions in terms of mode functions (2.44) (for fixed frequency  $\omega$ )

$$\Pi_u(0^-) = \Pi_d(0^+), \quad (2.46a)$$

$$\partial_x \Pi_u(0^-) = \partial_x \Pi_d(0^+). \quad (2.46b)$$

Here  $0^\pm$  denotes the limit  $x \rightarrow 0$  taken from above and from below respectively.

### 2.3.4 The scattering solution

Looking at the possible combinations of (2.44), the ones we are interested in are the scattering modes. These are modes originating from infinity on a well defined in-going mode (either  $u|in$ ,  $d1|in$  or  $d2|in$ , cf. with dispersion relations in figure (2.1)), impinging on the horizon, and leaving again towards (minus) infinity as a superposition of transmitted and reflected modes. In this connection the  $u|out$ -mode leaving the horizon towards minus infinity corresponds to the actual Hawking emission. Note that at  $x = 0$  there has to be a potential step due to the step-like configuration in the coupling  $g$  (2.40), which makes scattering possible [17].

We label the scattering modes with capital letters according to their incoming channels, which also distinguishes them from the more general modes (2.44). In addition to the capital indices there is still the index  $r \in \{u, d\}$ , since the modes have different analytic expressions for each side of the horizon. Therefore the scattering modes are  $\Pi_r^U$ ,  $\Pi_r^{D1}$  and  $\Pi_r^{D2}$ . We will display the explicit expressions in the following [17]. One should note, that all the modes are  $x$ -dependent.

#### $U$ mode, initiated by $u|in$

$$\Pi_u^U = \pi_{u|in} + S_{u,u} \pi_{u|out} + S_{u,u}^{eva} \pi_{u|eva}, \quad (2.47a)$$

$$\Pi_d^U = S_{d1,u} \pi_{d1|out} + \Theta(\Omega^* - \omega) S_{d2,u} \pi_{d2|out} + \Theta(\omega - \Omega^*) S_{d2,u}^{eva} \pi_{d2|eva}. \quad (2.47b)$$

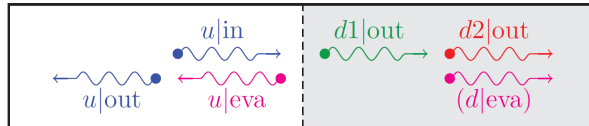
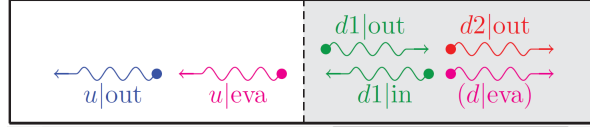


Figure 2.2:  $U$  scattering mode as a superposition of the eigenmodes, initiated by  $u|in$

**D1 mode, initiated by  $d1|in$** 

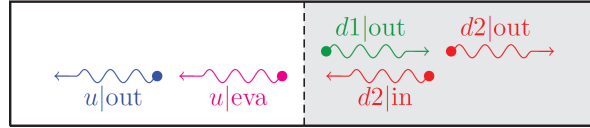
$$\Pi_u^{D1} = S_{u,d1}\pi_{u|out} + S_{u,d1}^{eva}\pi_{u|eva}, \quad (2.48a)$$

$$\Pi_d^{D1} = \pi_{d1|in} + S_{d1,d1}\pi_{d1|out} + \Theta(\Omega^* - \omega)S_{d2,d1}\pi_{d2|out} + \Theta(\omega - \Omega^*)S_{d2,d1}^{eva}\pi_{d|eva}. \quad (2.48b)$$

Figure 2.3: D1 scattering mode as a superposition of the eigenmodes, initiated by  $d1|in$ **D2 mode, initiated by  $d2|in$** 

$$\Pi_u^{D2} = \Theta(\Omega^* - \omega) \left[ S_{u,d2}\pi_{u|out} + S_{u,d2}^{eva}\pi_{u|eva} \right], \quad (2.49a)$$

$$\Pi_d^{D2} = \Theta(\Omega^* - \omega) \left[ \pi_{d2|in} + S_{d1,d2}\pi_{d1|out} + S_{d2,d2}\pi_{d2|out} \right]. \quad (2.49b)$$

Figure 2.4: D2 scattering mode as a superposition of the eigenmodes, initiated by  $d2|in$ 

In figures 2.2 - 2.4 the scattering modes initiated by the three eigenmodes are displayed in a pictorial way [17]. The magenta wiggles represent the evanescent modes. While in the upstream region the  $u|eva$  mode is always one of the outgoing modes, the  $d|eva$  mode just replaces the  $d2|out$  if the energy is high enough ( $\omega > \Omega^*$ ). As mentioned above the analytic expressions are different for the up- or downstream region, but match at the horizon at  $x = 0$ .

The scattering coefficients are determined by solving the matching conditions (2.46a) and (2.46b), which together form a 4x4-system of linear equations. The full analytic expressions of the coefficients can be seen in [17]. They only depend on the frequency  $\omega$ . The square of the absolute values  $|S_{l',l}(\omega)|^2$  indicate the the transmission or reflection coefficient for an  $l$ -ingoing mode at frequency  $\omega$  (energy  $\hbar\omega$ ) into an  $l'$ -outgoing mode at the same frequency.

During the scattering process the energy has to be conserved, for that reason the  $S$ -matrix

$$\mathbf{S}(\omega) = \begin{pmatrix} S_{u,u} & S_{u,d1} & S_{u,d2} \\ S_{d1,u} & S_{d1,d1} & S_{d1,d2} \\ S_{d2,u} & S_{d2,d1} & S_{d2,d2} \end{pmatrix}, \quad (2.50)$$

has to obey the skew unitarity condition

$$\mathbf{S}^\dagger \eta \mathbf{S} = \eta = \mathbf{S} \eta \mathbf{S}^\dagger. \quad (2.51)$$

In this connection the unity matrix is replaced by the Bogoliubov metric

$\eta = \text{diag}(1, 1, -1)$ , due to the negative norm of the  $d2$ -modes.

If we are above the critical frequency  $\omega > \Omega^*$ , the stated  $3 \times 3$ -matrix (2.50) reduces to a  $2 \times 2$ -matrix

$$\mathbf{S} = \begin{pmatrix} S_{u,u} & S_{u,d1} \\ S_{d1,u} & S_{d1,d1} \end{pmatrix}, \quad (2.52)$$

which fulfils the usual unitarity condition

$$\mathbf{S}^\dagger \mathbf{S} = \mathbb{1} = \mathbf{S} \mathbf{S}^\dagger. \quad (2.53)$$

In this case, the  $D2$ -scattering mode does not exist anymore, because there cannot be a  $d2|_{\text{in}}$ -mode initiating the scattering. Furthermore the  $d2|_{\text{out}}$ -mode is replaced by the  $d2|_{\text{eva}}$ -mode. As one can see in equations (2.47) - (2.49), this is ensured by the Heavyside step functions  $\Theta(\Omega^* - \omega)$  and  $\Theta(\omega - \Omega^*)$ .

Alternatively, we also could put the expressions (2.50) and (2.52) of the  $S$ -matrix together by simply adding the factor  $\Theta(\Omega^* - \omega)$  to both, the third row and the third column. This will be helpful in the next section talking about density correlations.

Since the evanescent modes decay exponentially, they carry no current. For this reason the coefficients  $S_{i,j}^{\text{eva}}$  are neither involved in the unitary conditions (2.51) and (2.53), nor in the  $S$ -matrix itself.

In figure 2.5 the scattering coefficients as a function of the frequency  $\omega$ . For the case  $\omega > \Omega^*$  the transmission (and reflection) coefficients  $|S_{u,d1}|^2$  and  $|S_{d1,u}|^2$  ( $|S_{u,u}|^2$  and  $|S_{d1,d1}|^2$ ) show the usual behaviour expected in wave mechanics. They are between 0 and 1 and increase (decrease) with  $\omega$ . If the frequency falls below the critical frequency,  $\omega < \Omega^*$ , the statements made for the case  $\omega > \Omega^*$  are not valid anymore. Moreover the  $d2$ -modes are involved in the dynamics. As one can see in figure 2.5, all the coefficients  $|S_{i,d1}|^2$  and  $|S_{i,d2}|^2$  ( $\propto \omega^{-\frac{1}{2}}$ ) diverge in the low- $\omega$  limit. These divergences do not violate energy conservation because of the skew unitarity of the  $S$ -matrix. This is one of the main consequences of the occurrence of a horizon, which is the analogue to an

---

infinite surface gravity. For low energies the quasiparticles entering the system from the downstream region ( $d1|in$  or  $d2|in$ ) remain blocked at the horizon forever. Although these modes are blocked, at the horizon they partially transfer their energy which results in the  $u|out$  leaving the horizon.

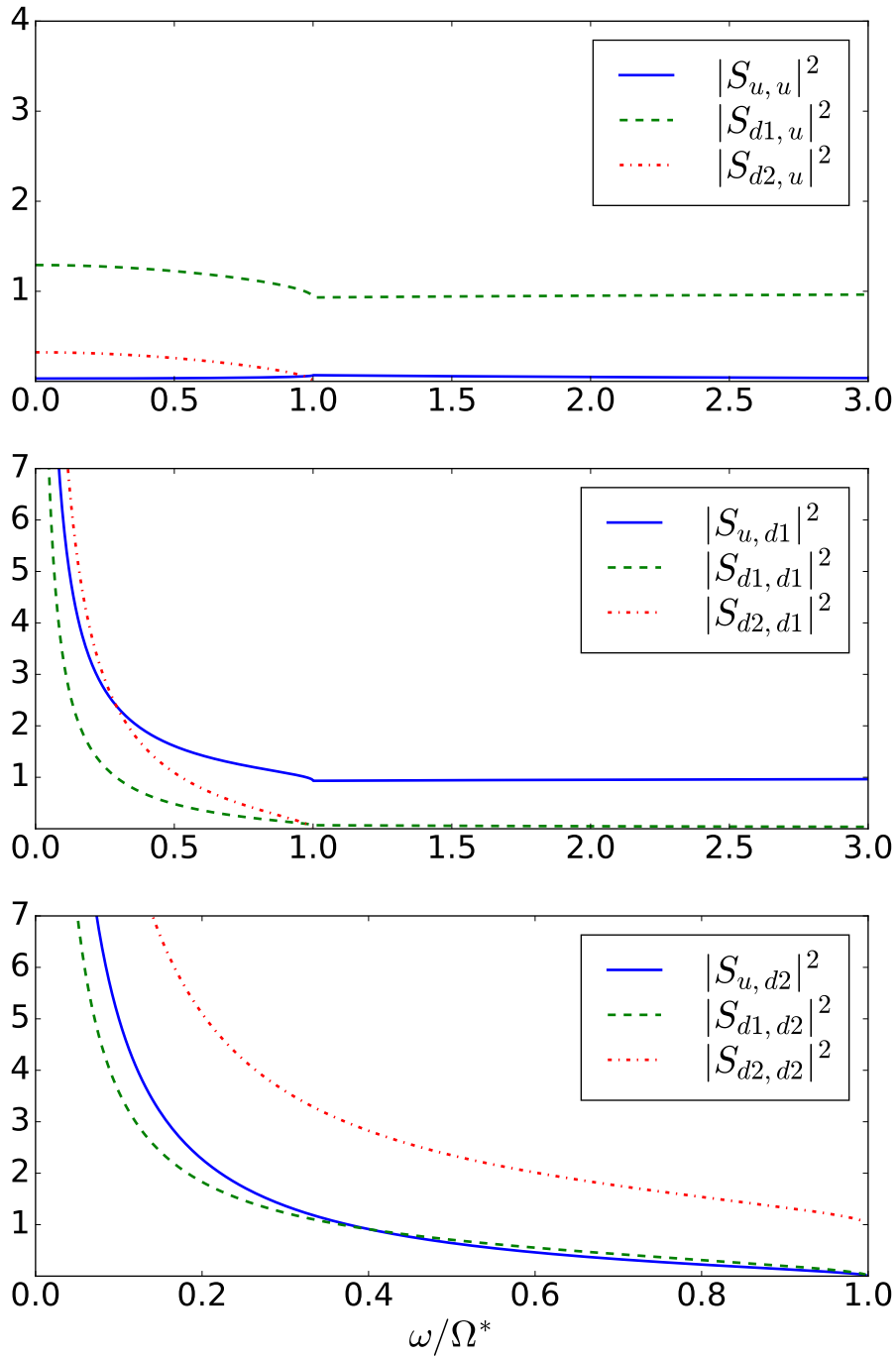


Figure 2.5: Transmission and reflection coefficient for the  $u|in$  mode (upper panel),  $d1|in$  mode (middle panel) and the  $d2|in$  mode (lower panel). The parameters used are  $g_u = 0.8$ ,  $g_d = 0.04$ ,  $v/c_u = 0.7$  and  $v/c_d = 3$ . For  $\omega/\Omega^* > 1$  the  $d2$  mode is not involved in scattering and the other coefficient show the usual behaviour. In the low  $\omega$  limit the coefficients for the  $d1|in$  and the  $d2|in$  mode diverge. This is the signature of an event horizon, [15].

### 2.3.5 Quantisation

After we investigated the scattering modes for our system in the past section, we are now able to expand our fields  $\delta\tilde{n}$  and  $\delta\tilde{\theta}$  in these scattering modes. That is simply a change of basis in which the expansion takes place, since all the scattering modes are linear combinations of the eigenmodes (2.25). In order to reach the new expansion, we simply replace the eigenmodes  $f_L^\pm(x)$  from (2.25a) and (2.25b) with the scattering modes. Therefore we rewrite the modes displayed in (2.47) - (2.49) as following

$$\Pi_L(x) = \begin{pmatrix} f_L^+(x, \omega) \\ f_L^-(x, \omega) \end{pmatrix} := \begin{cases} \Pi_u^L(x, \omega), & \text{if } x \leq 0. \\ \Pi_d^L(x, \omega), & \text{if } x > 0. \end{cases} \quad (2.54)$$

The index  $L \in \{U, D1, D2\}$  specifies which incoming channel is considered. The expansion now is

$$\begin{aligned} \delta\tilde{n}(x, t) &= \int_0^\infty \frac{d\omega}{\sqrt{2\pi}} \sum_{L \in \{U, D1\}} \left[ f_L^+(x, \omega) e^{-i\omega t} \hat{b}_L(\omega) + \left( f_L^+(x, \omega) \right)^* e^{i\omega t} \hat{b}_L^\dagger(\omega) \right] \\ &+ \int_0^{\Omega^*} \frac{d\omega}{\sqrt{2\pi}} \left[ f_{D2}^+(x, \omega) e^{-i\omega t} \hat{b}_{D2}^\dagger(\omega) + \left( f_{D2}^+(x, \omega) \right)^* e^{i\omega t} \hat{b}_{D2}(\omega) \right], \end{aligned} \quad (2.55a)$$

$$\begin{aligned} \delta\tilde{\theta}(x, t) &= -i \int_0^\infty \frac{d\omega}{\sqrt{2\pi}} \sum_{L \in \{U, D1\}} \left[ f_L^-(x, \omega) e^{-i\omega t} \hat{b}_L(\omega) - \left( f_L^-(x, \omega) \right)^* e^{i\omega t} \hat{b}_L^\dagger(\omega) \right] \\ &- i \int_0^{\Omega^*} \frac{d\omega}{\sqrt{2\pi}} \left[ f_{D2}^-(x, \omega) e^{-i\omega t} \hat{b}_{D2}^\dagger(\omega) - \left( f_{D2}^-(x, \omega) \right)^* e^{i\omega t} \hat{b}_{D2}(\omega) \right]. \end{aligned} \quad (2.55b)$$

In each of these expansions (2.55a) and (2.55b) the second integral has a cutoff at  $\omega = \Omega^*$ , which comes from the Heavyside step functions in equations (2.49).

The operators  $\hat{b}_L^\dagger(\omega)$  and  $\hat{b}_L(\omega)$  are now the creation and annihilation operators of an excitation of energy  $\hbar\omega$  in one of the three scattering modes  $U$ ,  $D1$  and  $D2$ . They obey the bosonic commutation relations

$$[\hat{b}_L(\omega), \hat{b}_{L'}^\dagger(\omega')] = \delta_{L,L'} \delta(\omega - \omega'), \quad (2.56a)$$

$$[\hat{b}_L(\omega), \hat{b}_{L'}(\omega')] = 0 = [\hat{b}_L^\dagger(\omega), \hat{b}_{L'}^\dagger(\omega')]. \quad (2.56b)$$

One also has to note, that for the  $D2$  scattering mode the quantisation is carried out in a nonstandard way. The role of the creation and annihilation operator is exchanged compared to the  $U$  and  $D1$  scattering mode. This has to do with the negative norm of the initiating  $d2|in$ -mode. Using the skew unitarity condition (2.51), one can show this

---

choice of quantisation is necessary for the commutation relation (2.6) to be fulfilled, [17].

The expression of our fields in terms of the scattering modes are now well suited for the investigation of density correlations in the next section.

### 3 Density correlations

As seen in [13], the two point density correlation was found to be the most suitable tool for identifying acoustic Hawking radiation.

In the one component Bose condensate the two point density correlation function is defined as

$$g^{(2)}(x_1, x_2) := \langle \psi^\dagger(x_1, t) \psi^\dagger(x_2, t) \psi(x_1, t) \psi(x_2, t) \rangle - \langle \psi^\dagger(x_1, t) \psi(x_1, t) \rangle \langle \psi^\dagger(x_2, t) \psi(x_2, t) \rangle. \quad (3.1)$$

By using  $\psi^\dagger(x_1, t) \psi(x_1, t) = n(x_1, t)$  and the commutation relation (2.2), equation (3.1) can be brought into the form

$$g^{(2)}(x_1, x_2) := \langle n(x_1, t) n(x_2, t) \rangle - \langle n(x_1, t) \rangle \delta(x_1 - x_2) - n_0^2 = \langle \delta n(x_1) \delta n(x_2) \rangle - n_0 \delta(x_1 - x_2), \quad (3.2)$$

where we inserted the mean field approximation (2.8) to get the second line, and additionally used

$$\langle \delta n(x, t) \rangle = 0, \quad (3.3)$$

per definition of the mean field. The delta function arises due to the commutator of  $\psi$  and  $\psi^\dagger$ , but we will focus on the correlation of the fluctuations. Using our expansion over the scattering modes (2.55a) we can rewrite the two point function (3.2) in terms of an integral over the frequency  $\omega$

$$g^{(2)}(x_1, x_2) = \int_0^\infty \frac{d\omega}{2\pi} \gamma(x_1, x_2, \omega) - n_0 \delta(x_1 - x_2). \quad (3.4)$$

Looking at the expression of  $\gamma(x_1, x_2, \omega)$ , one can see that there is a zero temperature contribution as well as a thermal one to  $\gamma(x_1, x_2, \omega)$ , where only the thermal part depends on the occupation number  $\mathcal{N}_L(\omega) = \langle b_L^\dagger(\omega) b_L(\omega) \rangle$ . Therefore we have

$$\gamma(x_1, x_2, \omega) = \gamma_0(x_1, x_2, \omega) + \gamma_{\text{th}}(x_1, x_2, \omega), \quad (3.5)$$

with

$$\gamma_0(x_1, x_2, \omega) = \sum_{L \in \{U, D1\}} f_L^+(x_1) \left( f_L^+(x_2) \right)^* + \left( f_{D2}^+(x_1) \right)^* f_{D2}^+(x_2) \quad (3.6)$$

and

$$\gamma_{\text{th}}(x_1, x_2, \omega) = \sum_{L \in \{U, D1, D2\}} \left[ f_L^+(x_1) \left( f_L^+(x_2) \right)^* + \left( f_L^+(x_1) \right)^* f_L^+(x_2) \right] \times \mathcal{N}_L(\omega). \quad (3.7)$$

The zero-temperature contribution stays finite even if  $T = 0$ . In this case the occupation number  $\mathcal{N}_L(\omega) = 0$ , as a consequence the thermal part  $\gamma_{\text{th}}(x_1, x_2, \omega)$  vanishes.

We will mainly focus on the  $T = 0$  case, therefore we only take a look at  $\gamma_0(x_1, x_2, \omega)$ . Since we are only considering density correlations only the first component of the scattering modes (2.47) - (2.49) is relevant for now. With the expressions for the mode functions from (2.25b) we are able to give the explicit expressions for  $\gamma_0(x_1, x_2, \omega)$ . In this treatise we restrict ourselves to the case where  $x_1$  and  $x_2$  are far away from the horizon. This allows us to neglect the evanescent modes in equations (2.47) - (2.49).

**1st case:  $x_1$  and  $x_2$  are both deep in the upstream region,  $x_1, x_2 \ll -\xi_u$**

$$\begin{aligned} \gamma_0(x_1, x_2, \omega) &= |F_{u|\text{in}}^+|^2 e^{ik_u|\text{in}(x_1-x_2)} + |F_{u|\text{out}}^+|^2 e^{ik_u|\text{out}(x_1-x_2)} \\ &+ \Theta(\Omega^* - \omega) \left[ |S_{u,d2}|^2 |F_{u|\text{out}}^+|^2 e^{ik_u|\text{out}(x_1-x_2)} + c.c. \right], \end{aligned} \quad (3.8)$$

where we used

$$|S_{u,u}|^2 + |S_{u,d1}|^2 = 1 + \Theta(\Omega^* - \omega) |S_{u,d2}|^2. \quad (3.9)$$

This comes from the skew unitarity condition (2.51) of the  $S$ -matrix (2.50).

**2nd case:  $x_1$  is deep in the upstream region and  $x_2$  is deep in the downstream region,  $x_1 \ll -\xi_u$  and  $x_2 \gg \xi_d$**

$$\begin{aligned} \gamma_0(x_1, x_2, \omega) &= \Theta(\Omega^* - \omega) \left[ |S_{u,d2}(S_{d1,d2})^* F_{u|\text{out}}^+(F_{d1|\text{out}}^+)^* e^{i(k_u|\text{out}x_1 - k_{d1|\text{out}}x_2)} \right. \\ &+ \left. |S_{u,d2}(S_{d2,d2})^* F_{u|\text{out}}^+(F_{d2|\text{out}}^+)^* e^{i(k_u|\text{out}x_1 - k_{d2|\text{out}}x_2)} + c.c. \right], \end{aligned} \quad (3.10)$$

where we again made use of the skew unitarity condition (2.51) of the  $S$ -matrix (2.50)

$$S_{u,u}(S_{d1,u})^* + S_{u,d1}(S_{d1,d1})^* = \Theta(\Omega^* - \omega)S_{u,d2}(S_{d1,d2})^*, \quad (3.11a)$$

$$S_{u,u}(S_{d2,u})^* + S_{u,d1}(S_{d2,d1})^* = \Theta(\Omega^* - \omega)S_{u,d2}(S_{d2,d2})^*. \quad (3.11b)$$

There is also the case where  $x_1$  is deep in the downstream region and  $x_2$  deep in the upstream region. Obviously this corresponds to the exchange  $x_1 \leftrightarrow x_2$ .

**3rd case:  $x_1$  and  $x_2$  are both deep in the downstream region,  $x_1, x_2 \gg \xi_d$**

$$\begin{aligned} \gamma_0(x_1, x_2, \omega) = & |F_{d1|in}^+|^2 e^{ik_{d1|in}(x_1-x_2)} + |F_{d1|out}^+|^2 e^{ik_{d1|out}(x_1-x_2)} \quad (3.12a) \\ & + \Theta(\Omega^* - \omega) \left[ |F_{d2|in}^+|^2 e^{ik_{d2|in}(x_1-x_2)} - |F_{d2|out}^+|^2 e^{ik_{d2|out}(x_1-x_2)} \right. \\ & + |S_{d1,d2}|^2 |F_{d1|out}^+|^2 e^{ik_{d1|out}(x_1-x_2)} + |S_{d2,d2}|^2 |F_{d2|out}^+|^2 e^{ik_{d2|out}(x_1-x_2)} \\ & + S_{d1,d2}(S_{d2,d2})^* F_{d1|out}^+ (F_{d2|out}^+)^* e^{i(k_{d1|out}x_1 - k_{d2|out}x_2)} \\ & \left. + S_{d2,d2}(S_{d1,d2})^* F_{d2|out}^+ (F_{d1|out}^+)^* e^{i(k_{d2|out}x_1 - k_{d1|out}x_2)} \right], \end{aligned}$$

this time we used

$$|S_{d1,u}|^2 + |S_{d1,d1}|^2 = 1 + \Theta(\Omega^* - \omega)|S_{d1,d2}|^2, \quad (3.13a)$$

$$|S_{d2,u}|^2 + |S_{d2,d1}|^2 = -1 + |S_{d2,d2}|^2, \quad (3.13b)$$

$$S_{d1,u}(S_{d2,u})^* + S_{d1,d1}(S_{d2,d1})^* = S_{d1,d2}(S_{d2,d2})^*, \quad (3.13c)$$

$$(S_{d1,u})^* S_{d2,u} + (S_{d1,d1})^* S_{d2,d1} = (S_{d1,d2})^* S_{d2,d2}. \quad (3.13d)$$

As stated in [13], there are only local correlations ("short-range antibunching") if there is no transition from a subsonic to a supersonic flow, which means  $\gamma_0(x_1, x_2, \omega) = 0$  for the second case. In the presence of an acoustic horizon new long-range correlations appear ( $\gamma_0(x_1, x_2, \omega) \neq 0$ ), which can be led back to the emission of correlated phonons. These correlated phonons arise due to quantum fluctuations and propagate away from the horizon through the  $u|out$ ,  $d1|out$  and  $d2|out$  channels. This can be identified with the analogue Hawking emission. In the low  $k$  limit the group velocity of a phonon is approximately equal to the sound of speed  $c_{u,d}$ . Additionally, in the laboratory system

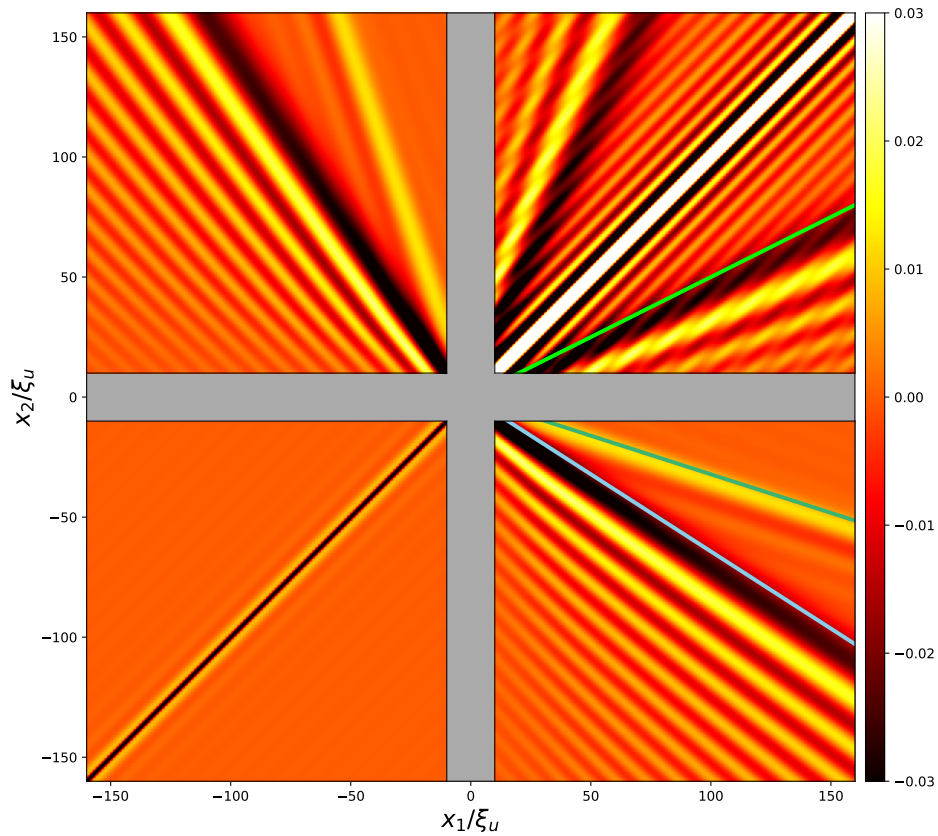


Figure 3.1: Plot for the dimensionless quantity  $\xi_u g^{(2)}$ , the parameters are the same as in figure 2.5. The grey area around the  $x_1$ - and  $x_2$ -axis corresponds to  $|x_1|, |x_2| < 10\xi_u$ . The coloured lines correspond to the largest expected long-range signals, the light green line corresponds to  $d2 - d1$  correlation, dark green corresponds to  $u - d1$  correlation and blue corresponds to  $u - d2$  correlation, [15].

the background flow velocity also has to be taken into account. Therefore at time  $t$  after the emission the phonons in the different channels are located at

$$x_{u|\text{out}}(t) = (v - c_u)t < 0, \quad (3.14a)$$

$$x_{d1|\text{out}}(t) = (v + c_d)t > 0, \quad (3.14b)$$

$$x_{d2|\text{out}}(t) = (v - c_d)t > 0, \quad (3.14c)$$

where the minus sign in front of  $c_d$ , in equation (3.14c), comes from the second real solution of the dispersion relation (2.16) for  $\omega < \Omega^*$ . Hence in the low  $k$  limit we expect the long-range correlation signals to appear along the lines of slope

$$\frac{x_{u|\text{out}}(t)}{x_{d1|\text{out}}(t)} = \frac{v - c_u}{v + c_d}, \quad (3.15a)$$

$$\frac{x_{u|\text{out}}(t)}{x_{d2|\text{out}}(t)} = \frac{v - c_u}{v - c_d}, \quad (3.15b)$$

$$\frac{x_{d2|\text{out}}(t)}{x_{d1|\text{out}}(t)} = \frac{v - c_d}{v + c_d}, \quad (3.15c)$$

for the  $u - d1$  correlation, the  $u - d2$  correlation and the  $d2 - d1$  correlation. Of course there are similar signals along the lines of inverse slope. This corresponds to the exchange  $x_1 \leftrightarrow x_2$ .

To summarise, provided that a transition from a subsonic to a supersonic flow takes place, the presence of such an acoustic horizon results long-range correlations, which correspond to the actual Hawking-effect. The numerical calculation of the correlation function matches the theoretical expectations regarding the largest correlation signals. The expected lines of slope are marked in figure 3.1 with coloured solid lines. If we take a closer look, we can observe a pattern parallel to the lines crossing the origin. This corresponds to a correlation of modes emitted at different times from the horizon.

## 4 Modifying the two component model

### 4.1 Bogoliubov theory of a two-component Bose Einstein condensate with opposite background flows

In this section we consider a system of two coupled Bose Einstein condensates in one spatial dimension. The problem described in section 2 is very similar with two components, as one can see in [10]. However, this time we consider the two components to have opposite background flows. The system is described by the following Hamiltonian:

$$\mathcal{H} = \int dx \left\{ \sum_{j=1,2} \psi_j^\dagger \left[ -\frac{1}{2m} \partial_x^2 + (V(x) - \mu) \right] \psi_j - J(\psi_1^\dagger \psi_2 + \psi_2^\dagger \psi_1) + \sum_{i,j=1,2} \frac{g_{ij}}{2} \psi_i^\dagger \psi_i \psi_j^\dagger \psi_j \right\}, \quad (4.1)$$

with an external potential  $V(x)$ , the chemical potential  $\mu$ , the tunnel coupling  $J$  and the inter and intra species coupling  $g_{ij}$ . For simplicity we set  $g_{11} = g_{22} = g$ ,  $g_{12} = g_{21} = \alpha g$  and assume that both components have equal atomic mass  $m$ . The bosonic annihilation and creation operators  $\psi_{1,2}$  and  $\psi_{1,2}^\dagger$  fulfil the usual commutation relations for fixed time

$$[\psi_i(x, t), \psi_j^\dagger(x', t)] = \delta_{ij} \delta(x - x'), \quad (4.2)$$

whilst all others vanish.

Following the same process as in section (2), we get a system of four coupled equations of motion for  $n_1, n_2, \theta_1$  and  $\theta_2$ :

$$\partial_t n_i = -\frac{1}{m} \partial_x [n_i \partial_x \theta_i] + 2J \sqrt{n_i n_j} \sin(\theta_i - \theta_j), \quad (4.3)$$

$$\partial_t \theta_i = \frac{1}{2m} \frac{\partial_x^2 \sqrt{n_i}}{\sqrt{n_i}} - \frac{1}{2m} (\partial_x \theta_i)^2 - [V(x) - \mu] + J \sqrt{\frac{n_j}{n_i}} \cos(\theta_i - \theta_j) - g n_i - \alpha g n_j \quad (4.4)$$

with  $i, j \in \{1, 2\}$  and  $i \neq j$ .

Again, we use the mean field approximation, slightly altered compared to section 2 by choosing different background phases  $\theta_{0i}(x)$  for each component

$$\begin{aligned} n_i(x, t) &= n_0(x) + \delta n_i(x, t), \\ \theta_i(x, t) &= \theta_{0i}(x) + \delta \theta_i(x, t) \end{aligned} \quad (4.5)$$

with

$$\begin{aligned}\theta_{01}(x) &= \frac{\pi x}{x_0}, \\ \theta_{02}(x) &= \pi - \frac{\pi x}{x_0}\end{aligned}\tag{4.6}$$

and

$$(n_0)_1 = (n_0)_2.\tag{4.7}$$

Therefore we get opposite signs for the background velocities for each component, which are defined as

$$v_i := \frac{\partial_x \theta_{0i}(x)}{m} = \pm \frac{\pi}{mx_0} := \pm v.\tag{4.8}$$

Linearising equations (4.3) and (4.4) we find to lowest order

$$\partial_x [n_0 v] = -2Jn_0 \sin\left(\frac{2\pi x}{x_0}\right) := -2Jn_0 \sin(ax)\tag{4.9}$$

which is the continuity equation, with a term on the r.h.s. depending on the tunnel coupling  $J$ . This holds for both components of the condensate. Looking at one component, we can see there are sources and sinks, since  $\sin(ax)$  can be both, positive and negative. Hence the particle number for one component is locally not conserved, unless the whole system with two components is considered. We also find the Gross-Pitaevskii equation

$$\left[ -\frac{1}{2m} \partial_x^2 + \frac{1}{2} m v^2 + V(x) - \mu + g n_0 (1 + \alpha) + J \cos(ax) \right] \sqrt{n_0} = 0.\tag{4.10}$$

Regarding the tunnel coupling  $J$ , we consider a slightly simplified setup. We divide our system into three parts, such that we have a region for  $x < 0$ ,  $0 \leq x \leq x_0$  and  $x_0 < x$ . In the following we call  $[0, x_0]$  the main area. Now we turn the tunnel coupling off in this main area. This is expressed by setting

$$J(x) = J\Theta(-x) + J\Theta(x - x_0)\tag{4.11}$$

and consequently

$$J(x) = 0 \quad \text{for} \quad x \in [0, x_0].\tag{4.12}$$

Thus our system forms a circulating current, where both components flow with opposite background velocities in one another and outside of the main area tunnel into each other.

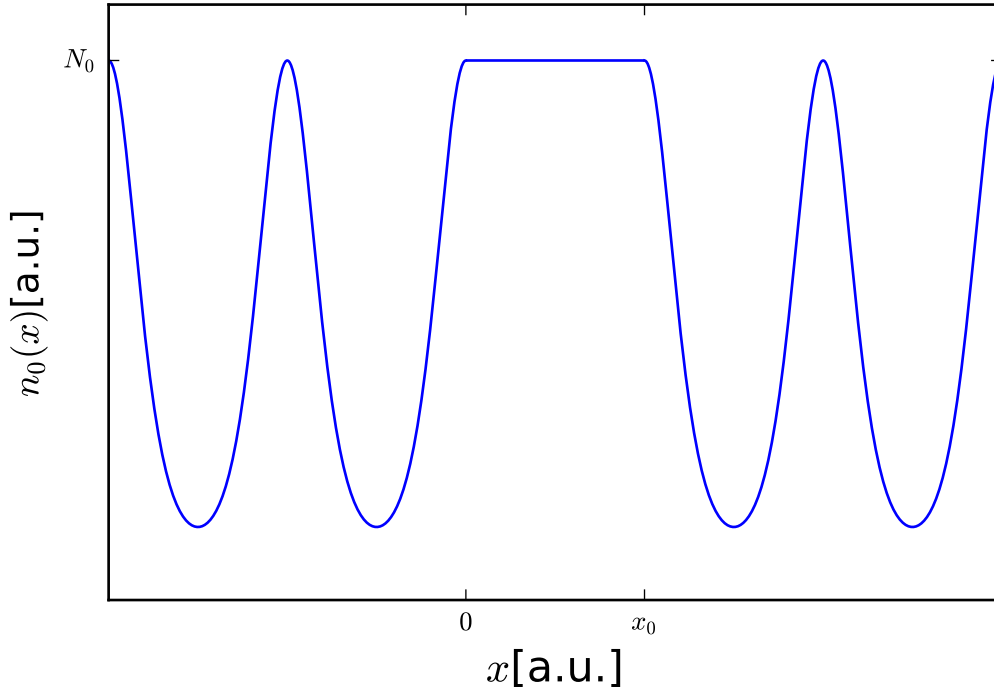


Figure 4.1: Background density  $n_0(x)$  for the three areas

Because of  $v = \text{const.}$  equation (4.9) is a differential equation of  $n_0 = n_0(x)$  for  $x \notin [0, x_0]$ . Solving (4.9), we get the background density profile for  $x \notin [0, x_0]$  for both components:

$$n_0(x) = \tilde{N}_0 \exp\left(\frac{2J}{va} \cos(ax)\right) \quad (4.13)$$

with  $\tilde{N}_0 = N_0 \exp\left(-\frac{2J}{va}\right)$ .

For the main area we have  $J = 0$ . We chose the background flow velocities  $\pm v$  to be constant. Therefore in order for the continuity equation (4.9) to be fulfilled the background density has to be constant for the main area,  $n_0(x) = N_0 = \text{const.}$  for  $x \in [0, x_0]$ . Therefore the condensate is homogeneous in the main area.

We transform our variables in order to investigate the symmetric (+) and antisymmetric (−) degrees of freedom

$$\delta n_+ = \delta n_1 + \delta n_2, \quad \delta n_- = \frac{\delta n_1 - \delta n_2}{2}, \quad (4.14a)$$

$$\delta \theta_+ = \frac{\delta \theta_1 + \delta \theta_2}{2}, \quad \delta \theta_- = \delta \theta_1 - \delta \theta_2. \quad (4.14b)$$

The symmetric and antisymmetric d.o.f. do not decouple instantly. We find to first order

$$\partial_t \delta n_+ = -\frac{2}{m} \partial_x [n_0 \partial_x \delta \theta_+] - 2v \partial_x \delta n_-, \quad (4.15a)$$

$$\partial_t \delta n_- = -\frac{1}{2m} \partial_x [n_0 \partial_x \delta \theta_-] - 2J n_0 a \cos(ax) \delta \theta_- - \frac{v}{2} \partial_x \delta n_+ - J \sin(ax) \delta n_+, \quad (4.15b)$$

$$\partial_t \delta \theta_+ = \frac{1}{2m} \frac{1}{4n_0} \partial_x \left[ n_0 \partial_x \left( \frac{\delta n_+}{n_0} \right) \right] - \frac{g}{2} (1 + \alpha) \delta n_+ - \frac{v}{2} \partial_x \delta \theta_- - J \sin(ax) \delta \theta_-, \quad (4.15c)$$

$$\partial_t \delta \theta_- = \frac{1}{2m} \frac{1}{n_0} \partial_x \left[ n_0 \partial_x \left( \frac{\delta n_-}{n_0} \right) \right] + \left[ \frac{J}{n_0} \cos(ax) - 2g(1 - \alpha) \right] \delta n_- - 2v \partial_x \delta \theta_+. \quad (4.15d)$$

In our main region these equations simplify a lot, because  $J = 0$  and  $n_0 = \text{const.}$ . Thus we get

$$\partial_t \delta n_+ = -\frac{2n_0}{m} \partial_x^2 \delta \theta_+ - 2v \partial_x \delta n_-, \quad (4.16a)$$

$$\partial_t \delta n_- = -\frac{n_0}{2m} \partial_x^2 \delta \theta_- - \frac{v}{2} \partial_x \delta n_+, \quad (4.16b)$$

$$\partial_t \delta \theta_+ = \frac{1}{2m} \frac{1}{4n_0} \partial_x^2 \delta n_+ - \frac{g}{2} (1 + \alpha) \delta n_+ - \frac{v}{2} \partial_x \delta \theta_-, \quad (4.16c)$$

$$\partial_t \delta \theta_- = \frac{1}{2m} \frac{1}{n_0} \partial_x^2 \delta n_- - 2g(1 - \alpha) \delta n_- - 2v \partial_x \delta \theta_+. \quad (4.16d)$$

In order to decouple (+) and (-) we have to manipulate equations (4.16a) - (4.16d). In the process we use the hydrodynamic approximation where we only keep first and second derivatives, higher ones are neglected.

First we take the time derivative of equation (4.16a) and insert equation (4.16b) (the time and the spatial derivative are interchangeable). Thus we get

$$\partial_t^2 \delta n_+ = -\frac{2n_0}{m} \partial_x^2 \partial_t \delta \theta_+ + v^2 \partial_x^2 \delta n_+. \quad (4.17)$$

For the other equation of the symmetric regime we take the time derivative of (4.16c) and insert (4.16d). We get

$$\partial_t^2 \delta \theta_+ = \frac{1}{8mn_0} \partial_x^2 \delta n_+ - \frac{g}{2} (1 + \alpha) \partial_t \delta n_+ + g(1 - \alpha) v \partial_x \delta n_- + v^2 \partial_x^2 \theta_+ \quad (4.18)$$

Now we isolate  $v \partial_x \delta n_-$  from equation (4.16a) and insert it in (4.18). This results in

$$\left[ \partial_t^2 - \left( v^2 - \frac{gn_0}{m} (1 - \alpha) \right) \partial_x^2 \right] \delta \theta_+ - \left[ \frac{1}{8mn_0} \partial_x^2 - g \right] \partial_t \delta n_+ = 0. \quad (4.19)$$

Following the same process we get the equations of motion for the antisymmetric regime. Summarised, our equations of motion decouple in the symmetric and antisymmetric d.o.f. and take the form

$$\left[ \partial_t^2 - v^2 \partial_x^2 \right] \delta n_+ + \frac{2n_0}{m} \partial_x^2 \partial_t \delta \theta_+ = 0, \quad (4.20a)$$

$$\left[ \partial_t^2 - \left( v^2 - \frac{gn_0}{m} (1 - \alpha) \right) \partial_x^2 \right] \delta \theta_+ - \left[ \frac{1}{8mn_0} \partial_x^2 - g \right] \partial_t \delta n_+ = 0, \quad (4.20b)$$

$$\left[ \partial_t^2 - v^2 \partial_x^2 \right] \delta n_- + \frac{n_0}{2m} \partial_x^2 \partial_t \delta \theta_- = 0, \quad (4.20c)$$

$$\left[ \partial_t^2 - \left( v^2 - \frac{gn_0}{m} (1 + \alpha) \right) \partial_x^2 \right] \delta \theta_- - \left[ \frac{1}{2mn_0} \partial_x^2 - 4g \right] \partial_t \delta n_- = 0. \quad (4.20d)$$

Once again we use the scaled variables  $\delta \tilde{n}_a = \frac{\delta n_a}{\sqrt{n_0}}$  and  $\delta \tilde{\theta}_a = \delta \theta_a \sqrt{n_0}$ ,  $a \in \{+, -\}$ . The equations (4.20a) - (4.20d) become

$$\left[ \partial_t^2 - v^2 \partial_x^2 \right] \delta \tilde{n}_+ + \frac{2}{m} \partial_x^2 \partial_t \delta \tilde{\theta}_+ = 0, \quad (4.21a)$$

$$\left[ \partial_t^2 - \left( v^2 - \frac{gn_0}{m} (1 - \alpha) \right) \partial_x^2 \right] \delta \tilde{\theta}_+ - \left[ \frac{1}{8m} \partial_x^2 - gn_0 \right] \partial_t \delta \tilde{n}_+ = 0, \quad (4.21b)$$

$$\left[ \partial_t^2 - v^2 \partial_x^2 \right] \delta \tilde{n}_- + \frac{1}{2m} \partial_x^2 \partial_t \delta \tilde{\theta}_- = 0, \quad (4.21c)$$

$$\left[ \partial_t^2 - \left( v^2 - \frac{gn_0}{m} (1 + \alpha) \right) \partial_x^2 \right] \delta \tilde{\theta}_- - \left[ \frac{1}{2m} \partial_x^2 - 4gn_0 \right] \partial_t \delta \tilde{n}_- = 0. \quad (4.21d)$$

As a result of decoupling the symmetric and antisymmetric d.o.f. in equations (4.16a) - (4.16d) we obtain four linear equations of motion which are second order in position and time. Having these, we are now able to derive the dispersion relation for both, the symmetric and antisymmetric regime.

## 4.2 Dispersion relation

Since we assumed our condensate to be homogeneous in the main area, we can expand the solutions of equations (4.21a) - (4.21d) in terms of plane waves

$$\delta \tilde{n}_+ = A e^{i(kx - \omega_+ t)}, \quad \delta \tilde{\theta}_+ = B e^{i(kx - \omega_+ t)}, \quad (4.22a)$$

$$\delta \tilde{n}_- = C e^{i(kx - \omega_- t)}, \quad \delta \tilde{\theta}_- = D e^{i(kx - \omega_- t)}. \quad (4.22b)$$

and insert them into equations (4.21a) - (4.21d). This leads to a matrix equation

$$\begin{pmatrix} -\omega_+^2 + v^2 k^2 & i\omega_+ \frac{2}{m} k^2 \\ -i\omega_+ \left[ \frac{1}{8m} k^2 + gn_0 \right] & -\omega_+^2 + \left[ v^2 - \frac{gn_0}{m} (1 - \alpha) \right] k^2 \end{pmatrix} \times \begin{pmatrix} A \\ B \end{pmatrix} = 0, \quad (4.23)$$

for the symmetric d.o.f. and

$$\begin{pmatrix} -\omega_-^2 + v^2 k^2 & i\omega_- \frac{1}{2m} k^2 \\ -i\omega_- [\frac{1}{2m} k^2 + 4gn_0] & -\omega_-^2 + [v^2 - \frac{gn_0}{m}(1 + \alpha)]k^2 \end{pmatrix} \times \begin{pmatrix} C \\ D \end{pmatrix} = 0, \quad (4.24)$$

for the antisymmetric d.o.f.

In order to have non trivial solutions for these matrix equations, the determinants have to vanish. This leads to the implicit dispersion relations

$$(\omega_+^2 - v^2 k^2)(\omega_+^2 - [v^2 - \frac{gn_0}{m}(1 - \alpha)]k^2) - \omega_+^2 \frac{1}{m} k^2 \left[ \frac{1}{4m} k^2 + 2gn_0 \right] = 0, \quad (4.25a)$$

$$(\omega_-^2 - v^2 k^2)(\omega_-^2 - [v^2 - \frac{gn_0}{m}(1 + \alpha)]k^2) - \omega_-^2 \frac{1}{m} k^2 \left[ \frac{1}{4m} k^2 + 2gn_0 \right] = 0. \quad (4.25b)$$

For both d.o.f. the dispersion only differs in the sign of the coupling parameter  $\alpha$ . Looking at the dispersion relations (4.25a) and (4.25b) we see that there are only terms proportional to  $\omega_a^4$ ,  $\omega_a^2$  and  $\omega_a^0$ . Therefore we can find a solution for  $\omega_a^2$ , namely

$$\omega_a^2 = -\frac{p_a}{2} \pm \sqrt{\left(\frac{p_a}{2}\right)^2 - q_a}, \quad (4.26)$$

with

$$p_a = -\frac{1}{4m^2} k^4 - \left[ 2v^2 + (1 + \alpha_a) \frac{gn_0}{m} \right] k^2 \quad \text{and} \quad q_a = \left[ v^2 - \frac{gn_0}{m}(1 - \alpha_a) \right] v^2 k^4, \quad (4.27)$$

with  $\alpha_a = +\alpha$  if  $a$  equals  $+$  and  $\alpha_a = -\alpha$  if  $a$  equals  $-$ .

As one can see, there two different branches in the dispersion relation (4.26) depending on the sign in front of the square root. We denote them by "+"- and "-"-branch. Since all parameters occurring in  $p_a$  are positive, it is clear that for the "+"-branch  $\omega_a^2 \propto k^4$  (leading order) and therefore diverges for large  $k$ , provided that the root exists (real value). This is similar to the standard Bogoliubov dispersion. More interesting is the "-"-branch. In order to investigate the large  $k$  limit, we absorb all the constants into new ones for simplicity. Introducing the new constant  $b$ ,  $c_a$ , and  $d_a$  we define

$$b := \frac{1}{4m^2}, \quad c_a := \left[ 2v^2 + (1 + \alpha_a) \frac{gn_0}{m} \right] \quad \text{and} \quad d_a := \left[ v^2 - \frac{gn_0}{m}(1 - \alpha_a) \right] v^2. \quad (4.28)$$

and therefore

$$p_a = -bk^4 - c_a k^2, \quad q_a = d_a k^4. \quad (4.29)$$

The "-"-branch of the dispersion (4.26) now reads

$$\begin{aligned}
\omega_a^2 &= \frac{1}{2}(bk^4 + c_a k^2) - \sqrt{\frac{1}{4}(bk^4 + c_a k^2)^2 - d_a k^4} \\
&= \frac{1}{2}(bk^4 + c_a k^2) - k^4 \sqrt{\frac{1}{4}(b + c_a k^{-2})^2 - d_a k^{-4}} \\
&:= \frac{1}{2}bk^4 + \frac{1}{2}c_a k^2 - k^4 f(k^{-1}).
\end{aligned} \tag{4.30}$$

In the last line we defined the function  $f$ , which is simply the square root term from the second line. Considering equation (4.30), more precisely  $f(k^{-1})$ , in the large  $k$  limit is equivalent to an expansion of  $f(x)$  for  $x \ll 1$ . This gives us

$$f(x) \approx \frac{1}{2}b + \frac{1}{2}c_a x^2 - \frac{d_a}{b} x^4 + \mathcal{O}(x^6). \tag{4.31}$$

Resubstituting  $k^{-1} = x$  and inserting this expansion in equation (4.30) leads to

$$\omega_a^2 = \frac{d_a}{b} + \mathcal{O}(k^{-6}). \tag{4.32}$$

For large  $k$  we can drop the terms of order  $(-6)$  and lower. Hence the frequency  $\omega_a$  approaches a limit frequency  $\omega_a^{\text{lim}}$  for  $k \rightarrow \infty$  with

$$\omega_a^{\text{lim}} = \sqrt{\frac{d_a}{b}} = 2mv \sqrt{v^2 - \frac{gn_0}{m}(1 - \alpha_a)}, \quad v^2 > \frac{gn_0}{m}(1 - \alpha_a). \tag{4.33}$$

It is remarkable that this limit mainly depends on the background flow velocity  $v$ . In figure 4.2 we plotted the dispersion relation for the main area. The "+"-branch is represented by the blue lines and shows the usual behaviour. The "-"-branch is represented by the green line and the asymptotic behaviour can be clearly observed. The dotted lines are the negative solutions of equation (4.30) if one takes the root. These are the negative norm branches, similar to the ones mentioned in section 2. They also can be seen as holes or anti particles, respectively.

In figure 4.3 we plotted the dispersion relation (4.30) for positive  $k$  and  $\omega$  over logarithmic axes. Here the power laws of the branches are well presented. Both are linear in the low  $k$  regime. At a certain value of  $k$  (around  $\sim 10^1$ ) the power laws become noticeably different. The "+"-branch becomes quadratic, similar to the Bogoliubov dispersion (2.16), whereas the "-"-branch manifestly shows constant behaviour. This is consistent with the expansion of equation (4.30) for large  $k$ . Roughly speaking, it means that if the frequency approximately reaches the limit frequency  $\omega_a^{\text{lim}}$ , there are infinitely many real solutions for  $k$ , which is not very intuitive. In the known setup involving

either only one component or two components having the same background flow velocity we always found a regular fourth order polynomial for the dispersion relation and therefore got four complex solutions for a fixed frequency  $\omega$  from which at least two solution were real. In our case, the energy of the modes for different  $k$  is somehow determined by the background velocity  $v$ .

At this point it has to be mentioned that it is difficult to define the speed of sound. So in general, as stated in [4], a modified dispersion relation can be written as

$$\Omega^2 = \omega_0 + c^2 k^2 + \eta k^4 + \dots \quad (4.34)$$

where  $\Omega^2$  is the co-moving frequency,  $\omega_0$  is proportional to an effective mass (rest mass) and  $c$  is the speed of sound.  $\eta$  contains higher order corrections which go beyond the hydrodynamic approximation. Here the first problem arises. The background flows of both components of the condensate point in opposite directions, hence it is not possible to Galilei-transform our system to a system at rest, contrary to the case where both backgrounds flow in the same direction. Because of that one cannot simply talk about a co-moving frequency. Secondly, we could identify  $\Omega^2$  from equation (4.34) with the frequency  $\omega_a^2(k)$  of the laboratory system. If we then expand the dispersion relation for small  $k$  and look at the coefficient of the term  $\propto k^2$ , we would have a speed of sound  $c_s = c_s(v^2)$  and hence it would be dependent on the square of the background flow velocity, which is not easy to handle. Therefore it remains unclear whether a transition from a subsonic to a supersonic flow can be reached. On top of that one cannot tune the background flow velocity arbitrarily high either, since it then can be predicted that the "-"-branch will disappear if  $\omega_a^2(k)$  becomes negative. Nevertheless we will take a close look at the dispersion relation itself, regarding the  $k$ -roots for a fixed frequency  $\omega_a > \omega_a^{\text{lim}}$ .

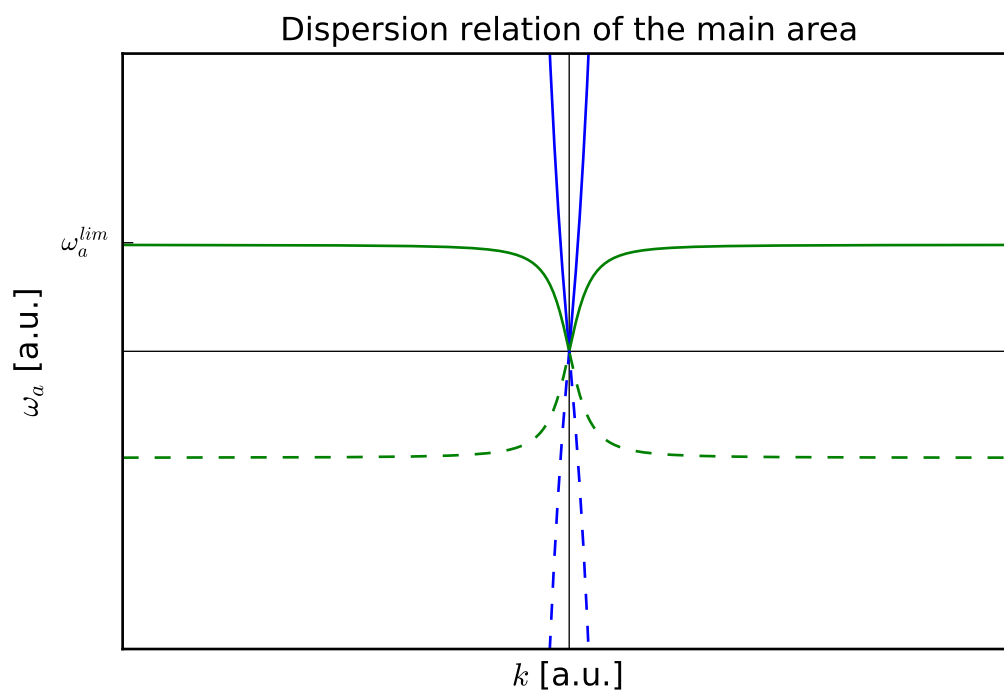


Figure 4.2: Positive and negative norm branches of the dispersion relation

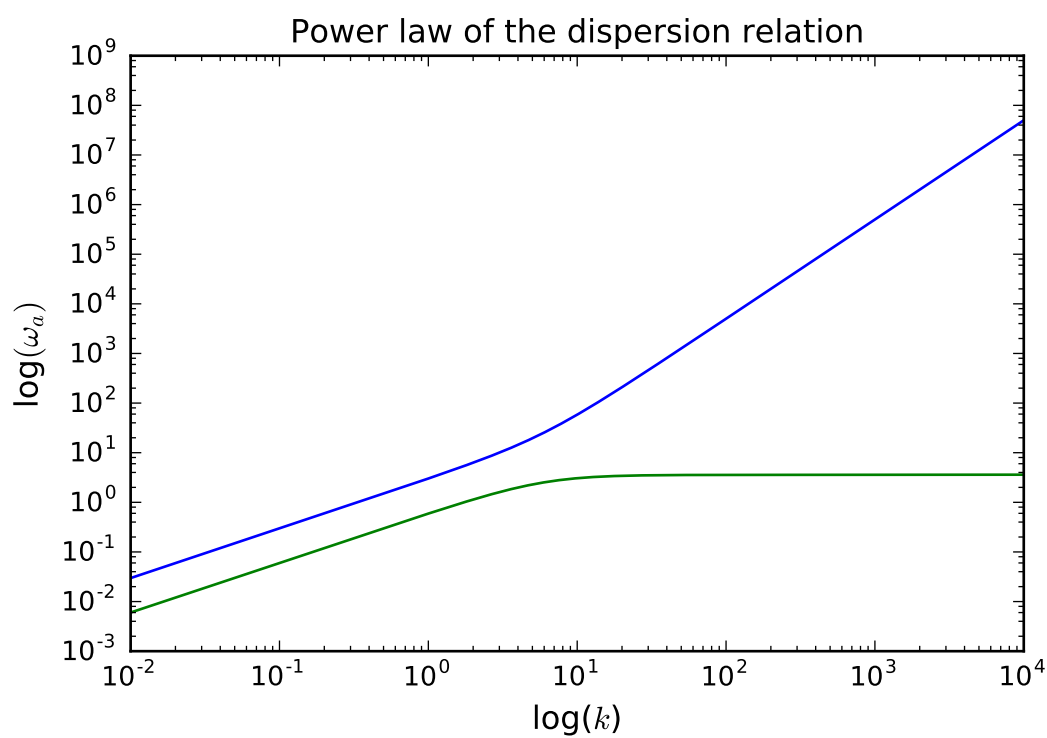


Figure 4.3: Double logarithmic plot of the "+"- and the "-"-branch

If we now consider a fixed frequency  $\omega$ , significantly below the critical frequency  $\omega_a^{\text{lim}}$ , there are four real solutions for  $k$ . This can be seen in figure 4.4. We have the two roots of the "+"-branch denoted by  $k^+$  and  $-k^+$ , which correspond to modes with positive and negative group velocity, respectively. We find analogue results for the roots  $k^-$  and  $-k^-$  in the "-"-branch. Above the critical frequency,  $\omega > \omega_a^{\text{lim}}$ , there are only the roots of the "+"-branch left. The other two solutions are now complex conjugate to each other, similar to the dispersion relation derived in section 2.

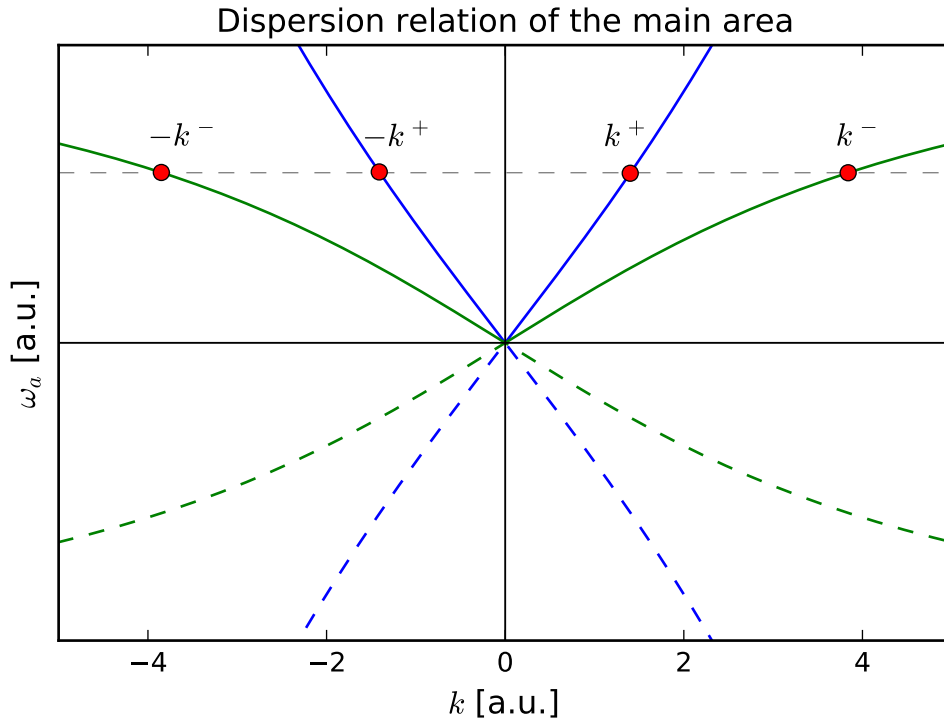


Figure 4.4: Four modes for a fixed frequency  $\omega$ , below the critical frequency  $\omega_a^{\text{lim}}$

For the parameters in the plots of figure 4.2 - 4.4 we used  $v = 2$  and  $\alpha = 0.2$ . The general structure of  $\omega_a(k)$  is conserved if we choose  $\alpha = -0.2$ , that is the behaviour for small and large  $k$  for each of the branches. This underlines that the symmetric and antisymmetric d.o.f. do not differ very much, which can be led back to opposite background flows and consequently the stronger coupling of both d.o.f..

## 5 Conclusion

In this thesis we first considered a one dimensional Bose Einstein condensate. We made use of the Bogoliubov approach and investigated the fluctuations to the first order.

By making an appropriate choice for the coupling constant  $g$  we reached a system containing an acoustic horizon which corresponds to transition from a subsonic to a supersonic background flow. Hence there is an upstream and a downstream region, in which the dispersion relation we derived shows different behaviour.

From our equations of motion we deduced the matching conditions for our fields at the horizon, which resulted in matching conditions for the eigenmodes of the whole system. To this end we used the Bogoliubov expansion.

Among these eigenmodes for the whole system, we focused on the scattering modes and presented their explicit expressions. Finally our fields could be expanded in these scattering modes, which was crucial for the following step.

Investigating the density correlations, we considered the outgoing modes to be emitted at the same time from the horizon. We found that beside the expected short range correlation, there is also a long-range correlation signal, which is a direct consequence of the occurrence of an horizon. This can be identified with the analogue Hawking-effect. The numerical calculation of the correlation function shows a behaviour which is similar to the (theoretical) expectations. This is clarified by the three dimensional plot of the correlation function in figure 3.1.

In the fourth section we considered a two component Bose Einstein condensate, where each of the component has a background flow velocity pointing in opposite directions. We wanted to investigate whether in this configuration a Hawking-like effect arises. To this end we decoupled our equations of motion and derived the dispersion relation once again. In this connection we transformed our variables to symmetric and antisymmetric degrees of freedom. Under certain approximations this made the decoupling possible in the first place.

It turned out that it is not trivial to read off the speed of sound from the dispersion relation which makes it difficult to set an upstream and a downstream region. Furthermore the dispersion was not skewed by the background flow velocity  $v$  the way it was in the case of an one component flow. This leads us to conclude that it is rather unlikely to observe a Hawking-like effect.

If the frequency  $\omega$  approaches a critical frequency, nearly infinite modes can be occupied. It is nonphysical that modes with an arbitrary high wave number  $k$  have the same probability to be occupied as the lower ones for a given frequency  $\omega$  near to the critical frequency  $\omega_a^{\text{lim}}$ . Therefore we can conclude that the amplitude of these large  $k$  modes have to be suppressed somehow by other effects.

Moreover, the group velocity of these modes goes to zero for  $k \rightarrow \infty$ . For this reason, it is not very sensible to consider them in connection to emitted modes or emitted

radiation, respectively, since these are modes propagating away from the horizon. Nevertheless, this does not apply to the modes, whose frequency is significantly below the critical frequency. These would be the ones to work with if we consider scattering processes.

## 5.1 Outlook

We considered a setup where the tunnelling only takes place outside the main area. This simplified the equations of motion a lot inside the main area. If we consider  $J \neq 0$  throughout the whole system, the equations of motion retain the form seen in (4.15). In this case the degrees of freedom are strongly coupled and seem to be analytically unsolvable in an exact way. This is mainly caused by the potential terms containing  $\sin(x)$  and  $\cos(x)$ . Further one cannot use the plane wave approach to derive the dispersion relation. If we keep the division into three areas, where we tune the parameters (especially  $v$ ) significantly different in the main area, we could expand the potential terms near the edge of the main area and expand the solutions in Bessel-functions. From that we should probably be able to formulate matching conditions between each two of the three areas, namely at the "horizon"-like positions  $x = 0$  and  $x = x_0$ . These are needed if we follow a similar process as in section 2. Consequently scattering processes involving the modes presented in figure 4.4 could be investigated and hence correlation functions computed. Thereby one could make sure if actual Hawking-like effects occur.

Despite us not being able to verify an analogue Hawking-effect in our modified mode at this point, the results of this thesis, in particular the dispersion relation in equation (4.30), awakens scientific interest from another point of view. It is possible that application can be found in other areas, for instance in solid state physics. The resulting behaviour of one of the branches of the dispersion relation resembles a band structure which plays an important role if one studies the physics of crystalline materials. Hence it would be interesting if one makes further investigations regarding, e.g., Bose Einstein condensates in periodic potentials. However, a detailed study of this was out of scope for this work, and thus could be a potential topic for future research. Overall we can say, that by no means the calculations can be carried out in such a straightforward manner as was the case of the one component condensate. As an educated guess we believe that numerical tools are required, especially to handle the coupled equations of motion properly.



## **Acknowledgements**

I want to thank my supervisor Professor Thomas Gasenzer for fruitful conversations and interesting new considerations. I am also very grateful for my flatmate and friend Frederick del Pozo who gave me topic related as well as linguistic advice. I am very thankful to my parents who support me throughout the whole time studying physics and before. Last but not least special thanks to my bachelor buddy Jan Philipp Klinger who made the hours in the office much more enjoyable.

## References

- [1] S. W. Hawking. Particle creation by black holes. *Comm. Math. Phys.*, 43(3):199–220, 1975.
- [2] Carlos Barceló, Stefano Liberati, and Matt Visser. Analogue Gravity. *Living Reviews in Relativity*, 8(1):12, Dec 2005.
- [3] W. G. Unruh. Experimental black-hole evaporation? *Phys. Rev. Lett.*, 46:1351–1353, May 1981.
- [4] William Unruh and Ralf Schützhold. *Quantum Analogues: From Phase Transitions to Black Holes and Cosmology*. Springer, 2007.
- [5] Germain Rousseaux, Christian Mathis, Philippe Maïssa, Thomas G. Philbin, and Ulf Leonhardt. Observation of negative-frequency waves in a water tank: a classical analogue to the Hawking effect? *New Journal of Physics*, 10(5):053015, May 2008.
- [6] David Bermudez and Ulf Leonhardt. Hawking spectrum for a fiber-optical analog of the event horizon. , 93(5):053820, May 2016.
- [7] M. Elazar, V. Fleurov, and S. Bar-Ad. All-optical event horizon in an optical analog of a laval nozzle. *Phys. Rev. A*, 86:063821, Dec 2012.
- [8] Jeff Steinhauer. Observation of quantum Hawking radiation and its entanglement in an analogue black hole. *Nature Physics*, 12(10):959–965, Oct 2016.
- [9] Ulf Leonhardt. Questioning the recent observation of quantum Hawking radiation. *arXiv e-prints*, page arXiv:1609.03803, Sep 2016.
- [10] P. É. Larré and N. Pavloff. Hawking radiation in a two-component Bose-Einstein condensate. *EPL (Europhysics Letters)*, 103(6):60001, Sep 2013.
- [11] Sebastian Erne. Generalized gibbs ensemble for two linearly coupled quasicondensates. unpublished.
- [12] C. J. Pethick and H. Smith. *Bose–Einstein Condensation in Dilute Gases*. Cambridge University Press, 2 edition, 2008.
- [13] A. Recati, N. Pavloff, and I. Carusotto. Bogoliubov theory of acoustic hawking radiation in bose-einstein condensates. *Phys. Rev. A*, 80:043603, Oct 2009.
- [14] Roberto Balbinot, Iacopo Carusotto, Alessandro Fabbri, Carlos Mayoral, and Alessio Recati. *Understanding Hawking Radiation from Simple Models of Atomic Bose-Einstein Condensates*, volume 870, page 181. 2013.
- [15] Linda Angenoorth. Bogoliubov theory of quantum fluctuations around acoustic black hole horizons in a two component bose einstein condensate. Master thesis, 2017.
- [16] C. Barceló, A. Cano, L. J. Garay, and G. Jannes. Stability analysis of sonic horizons in bose-einstein condensates. *Phys. Rev. D*, 74:024008, Jul 2006.
- [17] P.-É. Larré, A. Recati, I. Carusotto, and N. Pavloff. Quantum fluctuations around black hole horizons in bose-einstein condensates. *Phys. Rev. A*, 85:013621, Jan 2012.

## **Eidesstattliche Erklärung**

Ich versichere, dass ich diese Arbeit selbstständig verfasst und keine anderen als die angegebenen Quellen und Hilfsmittel benutzt habe.

*Unterschrift :*

*Ort, Datum :*

